CAPITAL UNIVERSITY OF SCIENCE AND
TECHNOLOGY, ISLAMABAD

Acoustic Propagation and Scattering through Lined Cavities

by

Farhan Ahmad

A thesis submitted in partial fulfillment for the
degree of Master of Philosophy

in the

Faculty of Computing
Department of Mathematics

2021

I dedicate this effort to my Family, my dear Parents, my elegant Teachers and my supervisor Dr. Muhammad Afzal who are always source of inspiration for me and their contributions are uncounted.

CERTIFICATE OF APPROVAL

Acoustic Propagation and Scattering through Lined Cavities

by

Farhan Ahmad

(MMT193016)

THESIS EXAMINING COMMITTEE

S. No.	Examiner	Name	Organization
(a)	External Examiner	Dr. Mahmood ul Hassan	COMSATS, Islamabad
(b)	Internal Examiner	Dr. Rashid Ali	CUST, Islamabad
(c)	Supervisor	Dr. Muhammad Afzal	CUST, Islamabad

Dr. Muhammad Afzal
Thesis Supervisor
November, 2021

Dr. Muhammad Sagheer
Head
Dept. of Mathematics
November, 2021

Dr. Muhammad Abdul Qadir
Dean
Faculty of Computing
November, 2021

Author's Declaration

I, **Farhan ahmad** hereby state that my MPhil thesis titled "**Acoustic Propagation and Scattering through Lined Cavities**" is my own work and has not been submitted previously by me for taking any degree from Capital University of Science and Technology, Islamabad or anywhere else in the country/abroad.

At any time if my statement is found to be incorrect even after my graduation, the University has the right to withdraw my MPhil Degree.

(Farhan Ahmad)
Registration No: MMT193016

Plagiarism Undertaking

I solemnly declare that research work presented in this thesis titled "**Acoustic Propagation and Scattering through Lined Cavities**" is solely my research work with no significant contribution from any other person. Small contribution/help wherever taken has been duly acknowledged and that complete thesis has been written by me.

I understand the zero tolerance policy of the HEC and Capital University of Science and Technology towards plagiarism. Therefore, I as an author of the above titled thesis declare that no portion of my thesis has been plagiarized and any material used as reference is properly referred/cited.

I undertake that if I am found guilty of any formal plagiarism in the above titled thesis even after award of MPhil Degree, the University reserves the right to withdraw/revoke my MPhil degree and that HEC and the University have the right to publish my name on the HEC/University website on which names of students are placed who submitted plagiarized work.

(Farhan Ahmad)
Registration No: MMT193016

All Praises belong to Almighty Allah, Lord and the Creator of the universe Who bestowed upon me the courage and His countless blessings enabled me to accomplish my MPhil studies. He is the most Powerful, Gracious and Beneficent. My heartiest gratitude is to my respected supervisor **Dr. Muhammad Afzal** for invaluable and inspiring guidance and encouraging discussion which enabled me to complete my work successfully. His encouraging and instructive behaviour always motivated me to implement new ideas in my research work. May Allah blesses him with best. Thanks, also due to my chairman, Department of Mathematics Capital university of Science and Technology for providing necessary research facilities. I am highly indebted to my respectable teachers for their guidance during my course work. I am thankful to my best friends Muhammad Tanveer and Muhammad Faisal who helped me alot during this work directly or indirectly. Finally, I wish to thank my **family** members for continuous support, inspiration and encouragement, without whom I would never finish this thesis. My thanks go to my **parents** for the confidence and their love during all these years.

(Farhan Ahmad)

Abstract

In the present work the reflection and transmission through the chamber cavities including liners are analyzed. To explain the mechanism of Multimodal technique two prototype problems are discussed. These physical problems include rigid-rigid and rigid-impedance types of boundary conditions and are radiated by a plane piston. It is found that by changing the velocity of the piston a variation in scattering amplitudes is found. Further, to analyze the impact of acoustic liners in single and double cavities the Multimodal method is applied. The governing boundary value problems have excitation from the inlet and transmission from the ancheotic region. The absolute values of the amplitudes of reflected and transmitted modes are shown against frequency. From the numerical experiment, it is found that the liners as well as the addition of cavity effect on the sound attenuation.

Contents

List of Figures

Symbols

c	Speed of sound
C_p	Constant pressure
C_v	Constant volume
g	Gravitational acceleration
K	Dimensionless frequency
p	Instantaneous pressure
p_0	Equilibrium pressure
s	Condensation
T	Temperature
$\mathbf{u}$	Particle velocity of a fluid element
V	Velocity
ω	Frequency
ρ	Instantaneous density
ρ_0	Equilibrium density
∇	Divergence
∇p	Exerting force
τ	Ratio of specific heat
β	Bulk modulus
ξ	Orthonormal eigenfunction
δ	Kronecker delta
ψ	Orthogonal Function
γ	Eigenvalue of transverse modes
η	Wavenumber

Chapter 1

Introduction and Literature Review

1.1 Introduction

Acoustic liners [1] are used to reduce the noise emitting from Heating Ventilation and Air Conditioning (HVAC) systems of buildings, chimney stacks, powerstations, vehicles and aeroplanes. The frequently used acoustic liners are bulkreacting liners and locally reacting liners. Generally, the locally reacting liners are constructed by the perforated sheet of honeycomb layers that allow the propagation of waves normal to the duct wall. Locally reacting liners have the good absorption quality for small frequency range of noises. The main control of these liners are their validity and high potential of resistance. On the other hand, bulk reacting liners have broad absorption quality. These liners are composed of porous material and show less efficiency at lower frequency regime as compared with locally reacting liners. To control the low frequency range of noises, is infact a challenging issue.

The current work is related theoretical study of the reflection and transmission of acoustic waves in the channel containing reacting liners. The Multimodal scheme [17] is adopted to analyze the scattering behavior of incoming propagative modes

in the presence of locally reacting liners. The propagation of modes is linked with the eigenvalues and eigenvectors of transformed system. To ensure the accuracy of collected modes two simple duct problems are considered. First problem is bounded by rigid walls and is excited with a plane piston along the wall whereas, in the later problem the upper horizontal wall is replaced with impedance surface. Both of these problems are solved with Multimodal scheme. To analyze performance of physical system the model coefficients are ploted for different velocities of moving piston. The aforementioned worked is comprehensively discussed in Chapter 3. Wherease the effects of locally reacting liners in the cavities of the chamber are discussed in Chapter 4.

1.2 Literature Review

The propagation of sound waves in lined ducts having rigid walls have been discussed by many authors, for instance see [2, 3]. Various methods were preferred to study the propagation of sound waves in duct lined with locally reacting liners by using impedance condition. [4–16], Weiner-Hopf technique has been applied to diffraction from the objects having different material properties. These methods include: Multimodal method [17], Finite element method [18] and Point matching method [19]. Each approach has strength and limitations depending upon the considered model and the aims of investigations. Felix and Pagneux [20] assumed adiabatic lossy medium lined with reacting liners. In this paper, he considered the circular curved duct system and with the aid of Multimodal approach to investigate the impact of impedance wall conditions. Likewise, Bi et al. [21] assumed a circular rigid duct lined with a non-uniform reacting liners. The impedance condition assumed to be piece-wise constant across the duct boundary and the Multimodal method was used to sort the solution of the problem. They found that duct modes with rigid walls are linked with the eigenvalues and eigenfunctions of transformed system. The method fits well to analyze the vibrations having low, mid and high frequencies. The numerical results showed that the non-uniform liners have minor effects on the efficiency of this devise.

Auregan and Lerous [22] studied acoustically treated ducts are widely used in HVAC to reduce noise emission. The calculation of the acoustical propagation in such devices is, however, difficult because of the complexity of the sound interactions. Marx et al. [23] discussed that in the presence of flow, acoustic propagation is difficult to predict due to the diffraction of sound from sharp edges and joints. This is especially true in the region of the lined wall where there is turbulance in fluid flow. Shenderove [24] modeled that the sound field in a waveguide as the superposition of normal waves, whose mode shapes are deduced by the separation of variable technique. He postulated that a propagation in the positive direction can be expressed as the combination of function that are partial solutions to the Helmholt'z equation. Kirby [25] considered two different silencers of an exhaust system radiated from inlet pipe. He equiped the device with reactive and dissipative tools and concluded that the acoustic behavior of energy in silencers can be improved for higher frequency modes by reactive and dissipative materials.
Denia et al. [26] demonstrated that in the automotive exhaust system, dissipative silencers have been shown to provide desirable noise control. Because broad band sound attenuation occurs in the mid and high frequency ranges. Abom [27] discussed an expansion chamber including extensions from inlet and outlet duct regions to make it a structure of concentric ducts. The acoustic performance of a devise while considering uniform and reactive linings at the chamber's ends. The dispersion of waves through different layered media is discussed in [28–33]. Cummings and Chang [34] obtained the transmission loss of a dissipative expansion, chamber including the mean flow by a mode-matching technique. Xu et al. [35] developed a two dimensional analytical solution to examine the acoustic performance of dissipative expansion chamber by a pressure and velocity matching technique. Selamet et al. [36] investigated the effect of perforated ducts on the sound attenuation in dissipative silencers. Nawaz and Lawrie [37] and Nawaz et al. [38] discussed the sound scattering from structural discontinuity together with obstacles at finite junction. The continuity conditions of pressures and normal velocities at aperture are used to match the scattering modes. Afzal et al. [39] investigated the study of a devise comprises of a two dimensional reactive silencer in

which a membrane is attached to the internal walls of the expansion chamber and elastic plate is attached to the outlet duct parallel to the axis of the inlet/outlet. Accordingly, the mode-matching method has been applied to scattering problems in [40–50]. Lawrie [51] presented the class of orthogonality relations relevant to fluid-structure interaction.

Haung [52] analyzed drum like silencer and reflection of sound waves through chamber enclosed by vertical plates. Satti et al. [53] studied that the expansion chamber silencer that contains membrane bounded cavities and horizontal partitions inside of the expansion chamber. The surfaces of the splitting walls are assumed as rigid, soft, impedance or sound absorbing material. Rienstra [54] an alyzed the behavior of the acoustic modes of a lined channel with and without uniform mean flow, it appears that there are three types of modes: genuine acoustic modes, acoustic surface waves and hydrodynamic surface waves. Brambley and Peake [55] examined the behavior of the surface modes. It is well known that when the flow exists, the viscosity effects cannot be excluded especially near the walls. As a result, the boundary layer must be taken into account. Hassan and Rawlins [56] studied sound radiation by considering a trifurcated waveguide where the boundary conditions in the mathematical problem are of Robin type on some surfaces and rigid on the other surfaces.

Ayub et al. [57] presented a solution of the diffraction problem related to an acoustical trifurcated waveguide with mean flow consisting of hard and soft parallel planes and half-planes. Wang and Mak [58] investigated the sound wave propagation in a lined duct through periodic resonators array. The dissipation of waves in a discontinuous exible waveguide was discussed by Afzal et al. [59]. The use of acoustically absorbing liners to reduce noise in infinite closed ducts has been extensively documented in the literature, [60–62]. The generalised orthogonal properties of boundary value problems, including higher order boundary conditions, had been discussed by Lawrie and Abrahams [63]. They used the proposed scheme to explain acoustic scattering in membrane bounded ducts on prototype problems. Afzal and Satti [64] explored that the eigenfunction expansion forms of duct regions provide an appealing way to express field potentials.

Unknown mode amplitudes exist in these expansions, which can be determined by formulating the continuity conditions of normal velocities and pressures across regions at interfaces.

1.3 Thesis Structure

The present thesis include five chapters.

Chapter 1 contains introduction and literature survey relevant to work carried out in this thesis.

Chapter 2 comprises some basic definitions, physical laws and formulation of wave equation.

Chapter 3 contains the exploitation of rigid duct modes and liner duct modes. The conditions for liners are also placed in this chapter.

Chapter 4 have two problems. First contains a single cavity having liners in infinite waveguide while the second problem investigates the double lined cavities.

Chapter 5 provides the concluding remarks of the present study.

The references used in the thesis are mentioned in **Bibliography**.

Chapter 2

Preliminaries

This thesis contains physical problems that are relevant to the reflection, transmission and absorption of acoustic waves propagating in rectangular ducts or channels. The purpose of the present chapter is to discuss some basic terminologies which are useful in understanding the mathematical modelling and associated physical characteristics of the work presented in the rest of the chapters.

2.1 Waves

Wave is the disturbance in the medium which causes the particles of that medium to vibrate from one place to another to transfer the energy. It is important to know that waves transfer energy of the matter without transferring matter. Typical examples include light waves and sound waves etc.

2.2 Types of Waves

There are three types of waves based on the medium characteristics and energy propagation. These three types are:

• Mechanical waves

- Electromagnetic waves
- Matter waves

2.2.1 Mechanical Waves

Mechanical waves are the type of waves in which energy is transferred through the oscillations produced in a material medium. Waves produced on the strings and springs, waves produce on the water surface are some common examples. There are two types of mechanical waves.

- Longitudinal waves
- Transverse waves

Longitudinal Waves

Longitudinal waves are the waves in which direction of particles of medium are parallel to the direction of propagation of waves. Sound waves and pressure waves are some common examples of longitudinal waves.

Transverse Waves

If the direction of particles of medium are perpendicular to the direction of propagating waves then this type of waves are known as transverse waves. Examples of transverse waves are waves produce on slinky spring. Light also has properties of transverse waves although it is an electromagnetic waves.

2.2.2 Electromagnetic Waves

The waves which are created when electric and magnetic fields oscillate perpendicular to each other are known as electromagnetic waves. These are the only waves that do not need any material medium for the transfer of energy. These waves

travel in a vacuum with the same speed. The X rays, microwaves and radiowaves are some common examples of electromagnetic waves.

2.2.3 Matter Waves

Light has dual natures that is sometimes acts as radiation and sometime it acts as material which has momentum and which can strike with a force. The dual nature of light exist as both material and in wave form is known as matter waves.

2.3 Acoustics

Acoustics is the branch of science which deals with the propagation of mechanical waves in matter. This branch covers how sound energy emits, reflects and transmits through a medium. The term acoustics is derived from Greek word akoustikos which means to hear. Normal human frequency range of hearing lies between 20 Hz to 20k Hz. The vibrations with frequency less than 20 Hz is known as infra sound and greater than 20k Hz is ultra sound.

2.4 Acoustic Wave Equation

The acoustic propagation in certain medium can be described mathematically in term of equations, known as acoustic wave equation [65]. This equation can be derived from the physical laws of motion and equation of state. The derivation of acoustic wave equation is explained in the next subsections.

2.4.1 Conservation of Mass

The conservation of mass equation is related to the net flow of mass per volume per unit time to the instantaneous rate of change of mass density that is [65]

$$\frac{\partial \rho}{\partial t} + \nabla.(\rho \mathbf{u}) = 0, \tag{2.1}$$

where ρ is instantaneous mass density and $\mathbf{u}$ is the fluid particle velocity vector. The equation (2.1) is also known as equation of continuity.

2.4.2 Conservation of Momentum

The conservation of momentum states the net flow of momentum per volume per unit time to the forces acting on it [65]

$$\rho \left(\frac{\partial \mathbf{u}}{\partial t} + (\mathbf{u}.\nabla)\mathbf{u} \right) = -\nabla p + \rho \mathbf{g}, \tag{2.2}$$

where, p is the pressure and g is the gravitational acceleration . Also ∇p denotes the exerting force and $\rho \mathbf{g}$ shows the body force. With the aid of continuity equation (2.1), it is convenient to write

$$\rho \frac{D\mathbf{u}}{Dt} = -\nabla p + \rho \mathbf{g}, \tag{2.3}$$

where $D/Dt = \partial/\partial t + \mathbf{u} \cdot \nabla$ is the total time derivative known as Stokes total time derivatives [66] including first term to be time derivative and the second term is convective term.

2.4.3 Equation of State

The thermodynamic behaviour of the fluid can be expressed in term of an equation known as equation of state:

$$p = \rho r T \tag{2.4}$$

where p is the pressue in Pascal, T is temperature in Kelvin and r is the specific gas constant. A gas enclosed in a vessel having walls which are thermally conductive, the perfect gas isotherm can be written as:

$$\frac{p}{p_0} = \frac{\rho}{\rho_0}, \tag{2.5}$$

where p_0 and ρ_0 are the pressure and static density respectively. When no heat loss or gained by the system then perfect adiabatic is

$$\frac{p}{p_0} = \left(\frac{\rho}{\rho_0}\right)^{\tau}, \tag{2.6}$$

where τ is the ratio of specific heat at constant pressure C_p to the specific heat at constant volume i.e, $\tau C_p/C_v$. The condensation s, that yields change in density for given ambient fluid is define as

$$s = \frac{\rho - \rho_0}{\rho_0}, \tag{2.7}$$

or

$$\frac{p}{p_0} = (1+s)^{\tau}, \tag{2.8}$$

which leads to

$$p = p_0 \left\{1 + \tau s \frac{\tau(\tau-1)}{2!} s^2 + \cdots \right\}. \tag{2.9}$$

For linear relationship

$$p - p_0 \approx \tau p_0 s + O(s^2). \tag{2.10}$$

The relationship between density fluctuation and pressure can also be written by using Taylor's expansion as:

$$p = p_0 \left(\frac{\partial p}{\partial \rho}\right)_{\rho=\rho_0} (\rho - \rho_0) + \cdots, \tag{2.11}$$

or

$$p - p_0 \approx \rho_0 \left(\frac{\partial p}{\partial \rho}\right)_{\rho=-\rho_0} \frac{\rho - \rho_0}{\rho_0}, \tag{2.12}$$

or

$$p - p_0 \approx \rho_0 \left(\frac{\partial p}{\partial \rho}\right)_{\rho=-\rho_0} s + O(s^2). \tag{2.13}$$

By comparing equation (2.10) and (2.13), we get

$$\tau = \frac{\beta}{p_0}, \tag{2.14}$$

where $\beta = (\partial p/\partial \rho)_{\rho-\rho_0}$ is the adiabatic bulk modulus. The expression (2.13) after neglecting the higher order terms, takes form

$$p = \beta s. \tag{2.15}$$

2.4.4 Linearized Acoustic Wave Equation

For small condensation $s \ll 1$, the continuity equation can be linearized as:

$$\frac{\partial s}{\partial t} + \nabla \cdot (\rho \mathbf{u}) = 0. \tag{2.16}$$

Likewise linearized momentum equation in the absence of body forces

$$\rho_0 \frac{\partial \mathbf{u}}{\partial t} = -\nabla p \tag{2.17}$$

where $|\mathbf{u}.\nabla \mathbf{u}| \ll \partial \mathbf{u}/\partial t$ is neglected. Now by taking divergence of (2.17), we yield

$$\frac{\partial}{\partial t}(\nabla.\mathbf{u}) = -\frac{1}{\rho_0}\nabla^2 p. \tag{2.18}$$

Differentiating (2.18) with respect to t, we found

$$\frac{\partial^2 s}{\partial t^2} = -\frac{\partial}{\partial t}(\nabla.\mathbf{u}). \tag{2.19}$$

From (2.18) and (2.19), we obtain

$$\frac{\partial^2 s}{\partial t^2} = \frac{1}{\rho_0}\nabla^2 p. \tag{2.20}$$

On using (2.15), we get

$$\nabla^2 p = \frac{1}{c^2}\frac{\partial^2 p}{\partial t^2}, \tag{2.21}$$

where

$$c = (\beta/\rho_0)^{1/2}. \tag{2.22}$$

Equation (2.22) gives the speed of sound in fluid of density ρ, having bulk modulus β.

2.5 Multimodal Procedure

In order to solve the problem of waveguides with varying cross-section, modal methods have already been suggested several decades ago [67]. A detailed theoretical description of a modal decomposition approach and its application to several aeroacoustic problems have been provided during the 90s by Pagneux et al. In a nutshell, the idea of the multimodal approach as described in [68] is to express the local displacement field within the waveguide in a basis of guided wave modes of the corresponding waveguide with constant thickness at any given point along the direction of wave propagation. While similar mode expansions have been successfully applied in the investigation of wave propagation through waveguides of constant cross-section [69], the application to waveguides with varying cross-section is more complicated due to the fact that options for mode coupling and reflection have to be included into the model. With the continuous variation of cross-section being translated into a continuous variation of the coefficients describing relative weights within the expansion into the modal basis, the numerical effort of calculating the displacement field along the waveguide is now reduced to solving the differential equations which govern the evolution of these coefficients in wave propagation direction.

Chapter 3

Multimodal Solution Waveguide Containing Liner Cavities

In this chapter the propagation of acoustic waves radiated by plane piston lying along the vertical wall of duct is discussed. The boundary conditions of horizontal walls are assumed to be rigid-rigid and rigid-impedance. The Multimodal procedure [17] is adopted to determine the propagating modes in the duct region, which are then compared with the eigen modes found through the separation of variable method to verify the results. The boundary value problem relate Helmholt'z equation in accompanying with impedance and rigid type boundary conditions. Section 3.2 contains the mathematical modelling of wave propagation in rigid duct. The solution of the problem is found in Section 3.3. In Section 3.4, the modelling of the lined duct is discussed while its solution is explained in Section 3.5. The computational results and discussion is provided in Section 3.6.

3.1 Wave Propagation in Rigid Duct Radiated by Plane Piston

We consider the acoustic propagation in two-dimensional rectangular duct having boundaries at $\bar{y} = \bar{0}$ and $\bar{y} = \bar{a}$ as shown in Fig. 3.1. The inside of

the duct is filled with compressible fluid of density ρ and sound speed $\bar{c}$. The overbars here and henceforth denote the setting of dimensional variables.

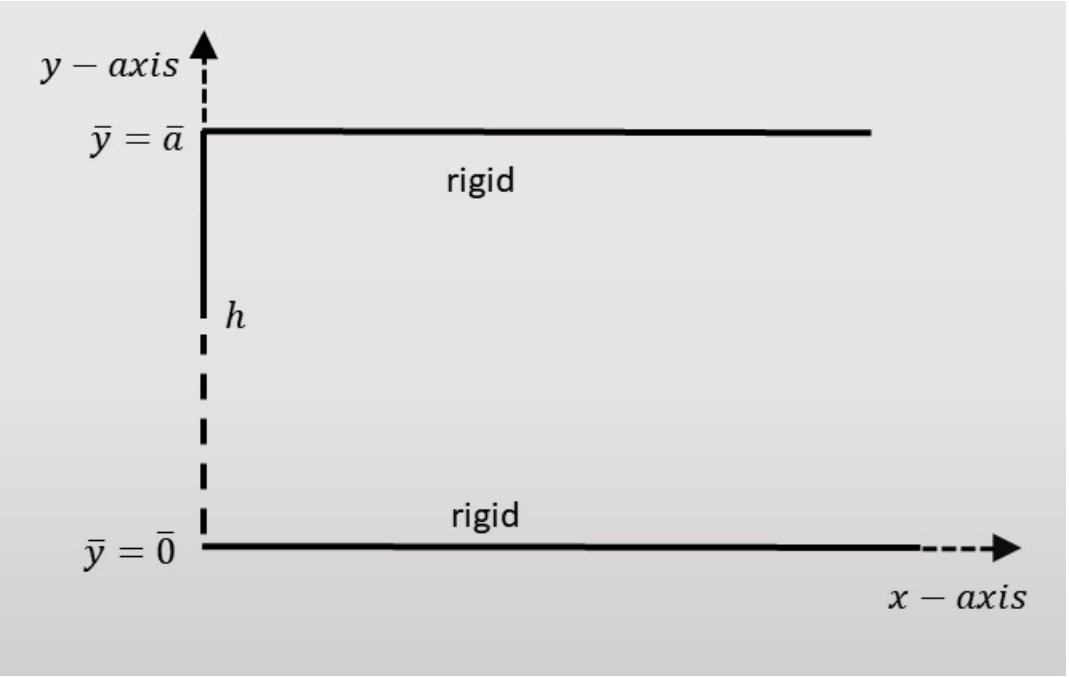

FIGURE 3.1: The physical configuration of duct.

The acoustic pressure $\bar{p}$ satisfies the dimensional wave equation

$$\nabla^2 \bar{P}(\bar{x}, \bar{y}, \bar{t}) = \frac{1}{\bar{c}^2} \frac{\partial^2 \bar{P}}{\partial \bar{t}^2}. \tag{3.1}$$

On assuming harmonic time dependence $e^{-i\bar{\omega}\bar{t}}$, where $\bar{\omega}$ is angular frequency, we can write

$$\bar{P}(\bar{x}, \bar{y}, \bar{t}) = \bar{p}(\bar{x}, \bar{y}) e^{-i\bar{\omega}\bar{t}}. \tag{3.2}$$

By using (3.2) into (3.1), we get the Helmholtz's equation

$$\left\{ \frac{\partial^2}{\partial \bar{x}^2} + \frac{\partial^2}{\partial \bar{y}^2} + \frac{\bar{\omega}^2}{\bar{c}^2} \right\} \bar{p}(\bar{x}, \bar{y}) = 0. \tag{3.3}$$

The duct walls can be rigid or impedance type. At rigid walls the normal velocity is zero

$$\hat{\boldsymbol{n}}.\overline{\boldsymbol{V}} = 0, \tag{3.4}$$

where $\hat{\boldsymbol{n}}$ is unit vector directed into the surface.

The relation between velocity $\bar{\boldsymbol{V}}$ and pressure $\bar{p}$ is

$$\frac{\partial \overline{\boldsymbol{V}}}{\partial \bar{t}} = -\nabla \bar{P}. \tag{3.5}$$

From the harmonic time dependence we can write

$$\overline{\boldsymbol{V}}(\bar{x}, \bar{y}, \bar{t}) = \bar{\boldsymbol{v}}(\bar{x}, \bar{y}) e^{-i\bar{\omega}\bar{t}}. \tag{3.6}$$

By invoking (3.2) and (3.6) into (3.3) and (3.4) we get

$$\hat{\boldsymbol{n}}.\bar{\boldsymbol{v}} = 0 \tag{3.7}$$

and

$$\bar{\boldsymbol{v}} = -\frac{i}{\bar{\omega}} \nabla \bar{p}. \tag{3.8}$$

On using (3.8) into (3.7) the rigid condition becomes

$$\hat{\boldsymbol{n}}.\nabla \bar{p} = 0. \tag{3.9}$$

We make the involving dimensionless variables through the transformations:

$$x = \frac{\bar{x}}{\overline{H}}, \quad y = \frac{\bar{y}}{\overline{H}}, \quad p = \frac{\bar{p}}{\rho \bar{c}^2}. \tag{3.10}$$

Here the variables without bars are in dimensionless form. On using the transformations, the nondimensional form of Helmholtz's equation and boundary condition becomes

$$\left\{ \frac{\partial^2}{\partial x^2} + \frac{\partial^2}{\partial y^2} + K^2 \right\} p(x, y) = 0 \tag{3.11}$$

and

$$\hat{\boldsymbol{n}}.\nabla p = 0, \tag{3.12}$$

where $K = \frac{\bar{\omega}\overline{H}}{\bar{c}}$, represent the dimensionless frequency.

3.2 Mathematical Formulation

The dimensionless form of boundary value problem is

$$\left\{\frac{\partial^2}{\partial x^2}+\frac{\partial^2}{\partial y^2}+K^2\right\}p(x,y)=0 \qquad 0<y<a, \tag{3.13}$$

$$\frac{\partial p}{\partial y}=0, \qquad y=0, \qquad x>0, \tag{3.14}$$

$$\frac{\partial p}{\partial y}=0, \qquad y=a, \qquad x>0, \tag{3.15}$$

$$\frac{\partial p}{\partial x}=0, \qquad x=0, \qquad h\leq y\leq a. \tag{3.16}$$

Consider the duct is radiated with a plane piston lying along vertical wall $0\leq y\leq h$ at $x=0$, moving with a constant velocity U, that gives

$$\frac{\partial p}{\partial x}=U, \qquad 0\leq y\leq h. \tag{3.17}$$

The propagation of waveforms in duct region is determined through Multimodal techniques [17] which is discussed in the next section.

3.3 Multimodal Solution

Consider incident radiation of acoustic waves propagation in duct towards positive x-direction. The travelling waves of guiding channel can be expressed as:

$$p(x,y)=\sum_{n=0}^{\infty}A_n\psi_n(y)e^{i\eta_n x}. \tag{3.18}$$

Here the quantity $\psi_n(y)$ determines the shape of n^{th} mode propagating towards positive x-direction having n^{th} mode wavenumber η_n and amplitude A_n. Apparently these quantities are unknowns. We may determine these unknowns with Multimodal procedure. By using (3.18) into (3.13) and using conditions (3.14)-(3.16), we get

$$\left\{\frac{d^2}{dy^2}+\gamma_n^2\right\}\psi_n(y)=0, \tag{3.19}$$

$$\psi_n'(0)=0, \tag{3.20}$$

$$\psi_n{}'(a)=0, \tag{3.21}$$

where $\gamma_n=\sqrt{K^2-\eta_n^2}$ and prime shows the differentiation with respect to involved variable. To project the solution of differential system (3.19)-(3.21), we formulate the corresponding eigenvalue problem

$$\frac{d^2\xi_n(y)}{dy^2}+\alpha_n^2\xi_n(y)=0, \tag{3.22}$$

$$\xi_n{}'(0)=0, \tag{3.23}$$

$$\xi_n{}'(a)=0. \tag{3.24}$$

On solving (3.22) subject to (3.23) and (3.24), we get the orthonormal eigenfunctions as:

$$\xi_n=\Lambda_n\cos(\alpha_n y); \quad n=0,1,2,\cdots \tag{3.25}$$

where $\alpha_n=n\pi/a, \quad n=0,1,2,\cdots$ are the eigenvalues.
Note the orthonormal functions ξ_n satisfy the relation

$$\int_0^a \xi_n(y)\xi_m(y)=\delta_{mn}, \tag{3.26}$$

where, δ_{mn} is kronecker delta

$$\delta_{mn}=\begin{cases}1 & m=n,\\ 0 & m\neq 0.\end{cases}$$

To project the solution of (3.19)-(3.21), we write $\psi_n(y)$ as the linear combination of orthonormal basis functions as:

$$\psi_n(y)=\sum_{m=0}^{\infty}B_{nm}\xi_{nm}(y)=\boldsymbol{\xi}^t\boldsymbol{B}, \tag{3.27}$$

where

$$\boldsymbol{\xi} = \begin{pmatrix} \xi_{n0} \\ \xi_{n1} \\ \vdots \\ \xi_{nm} \\ \vdots \end{pmatrix} \quad \text{and} \quad \boldsymbol{B} = \begin{pmatrix} B_{n0} \\ B_{n1} \\ \vdots \\ B_{nm} \\ \vdots \end{pmatrix}. \tag{3.28}$$

Note that superscript t in (3.28) of $\boldsymbol{\xi}$ represent the transpose of vector. On multiplying (3.19) with $\boldsymbol{\xi}$ and integrating over y from 0 to a, we get

$$\int_0^a \boldsymbol{\xi} \frac{d^2\psi_n}{dy^2} dy + \gamma_n^2 \int_0^a \boldsymbol{\xi}\psi_n dy = 0. \tag{3.29}$$

The solution of first integral of (3.29) can be obtained by performing integration by parts as:

$$\int_0^a \boldsymbol{\xi} \frac{d^2\psi_n}{dy^2} dy = \left(\boldsymbol{\xi}(y)\frac{d\psi_n}{dy}\right)\Big|_0^a - \left(\frac{d\boldsymbol{\xi}}{dy}\psi_n\right)\Big|_0^a + \int_0^a \psi_n \frac{d^2\boldsymbol{\xi}}{dy^2} dy. \tag{3.30}$$

On using boundary conditions (3.20)-(3.21) and (3.23)-(3.24), we get

$$\int_0^a \boldsymbol{\xi} \frac{d^2\psi_n}{dy^2} dy = \int_0^a \psi_n \frac{d^2\boldsymbol{\xi}}{dy^2} dy. \tag{3.31}$$

Therefore (3.29), takes the form

$$\int_0^a \psi_n \frac{d^2\boldsymbol{\xi}}{dy^2} dy + \gamma_n^2 \int_0^a \boldsymbol{\xi}\psi_n dy = 0. \tag{3.32}$$

On using (3.25) into (3.32), we find

$$-\int_0^a (\frac{m\pi}{a})^2 \boldsymbol{\xi}\psi_n dy + \gamma_n^2 \int_0^a \boldsymbol{\xi}\psi_n dy = 0, \tag{3.33}$$

or

$$-\int_0^a (\frac{m\pi}{a})^2 \xi_n\xi_m\psi_n dy + \gamma_n^2 \int_0^a \xi_n\xi_m\psi_n dy = 0. \tag{3.34}$$

Now on using (3.27) into (3.34), we obtain

$$-\int_0^a \sum_{p=0}^{\infty} \left(\frac{m\pi}{a}\right)^2 B_{np}\xi_{np}\xi_{nm}dy + \gamma_n^2 \int_0^a \sum_{p=0}^{\infty} B_{np}\xi_{np}\xi_{nm}dy, \tag{3.35}$$

or

$$-\left(\frac{m\pi}{a}\right)^2 \sum_{p=0}^{\infty} B_{np}\delta_{pm} + \gamma_n^2 \sum_{p=0}^{\infty} B_{np}\delta_{pm} = 0. \quad m = 0, 1, 2, \cdots \tag{3.36}$$

In a matrix form, (3.36) can be written as

$$-N_1 I\boldsymbol{B} + \gamma_n^2 I\boldsymbol{B} = 0, \tag{3.37}$$

where

$$N_1 = \begin{pmatrix} 0 & 0 & 0 & \dots & 0 \\ 0 & \frac{\pi^2}{a^2} & \vdots & \vdots & \vdots \\ \vdots & \vdots & \vdots & \vdots & \vdots \\ 0 & 0 & 0 & \frac{m^2\pi^2}{a^2} & \vdots \\ \vdots & \vdots & \vdots & \vdots & \vdots \end{pmatrix}. \tag{3.38}$$

Since $\gamma_n^2 = K^2 - \eta_n^2$, therefore (3.37) can be written as

$$\eta_n^2\boldsymbol{B} = N\boldsymbol{B}, \tag{3.39}$$

where

$$N = K^2 I - N_1. \tag{3.40}$$

Note that matrix N contain the eigenvalues η_n and eigenvectors X. The resulting field potential can be written as:

$$p(x, y) = \boldsymbol{\xi}^t[XD(x)\boldsymbol{A} + XD(-x)\boldsymbol{B}], \tag{3.41}$$

$$\boldsymbol{A}^t = \begin{bmatrix} A_0 & A_1 & \dots & A_n & \dots \end{bmatrix} \tag{3.42}$$

and

$$\boldsymbol{B}^t = \begin{bmatrix} \delta_{00} & \delta_{10} & \dots & \delta_{n0} & \dots \end{bmatrix}. \tag{3.43}$$

where

$$D(x) = \begin{pmatrix} e^{i\eta_0 x} & 0 & 0 & \dots & 0 & \dots \\ 0 & e^{i\eta_1 x} & 0 & \dots & 0 & \dots \\ \vdots & \vdots & e^{i\eta_2 x} & 0 & 0 & \dots \\ \vdots & \vdots & \vdots & \vdots & \vdots & \vdots \\ 0 & 0 & 0 & e^{i\eta_n x} & 0 & \dots \\ \vdots & \vdots & \vdots & \vdots & \vdots & \vdots \end{pmatrix}, \tag{3.44}$$

On differentiating (3.41) with respect to x, we find

$$\frac{\partial p}{\partial x} = \boldsymbol{\xi}^t [X \frac{d}{dx} D(x) \boldsymbol{A} + X \frac{d}{dx} D(-x) \boldsymbol{B}], \tag{3.45}$$

where

$$\frac{d}{dx} D(x)\Big|_{x=0} = \begin{pmatrix} i\eta_0 e^{i\eta_0 x} & 0 & 0 & \dots & 0 & \dots \\ 0 & i\eta_1 e^{i\eta_1 x} & 0 & \dots & 0 & \dots \\ \vdots & \vdots & i\eta_2 e^{i\eta_2 x} & 0 & 0 & \dots \\ \vdots & \vdots & \vdots & \vdots & \vdots & \vdots \\ 0 & 0 & 0 & i\eta_n e^{i\eta_n x} & 0 & \dots \\ \vdots & \vdots & \vdots & \vdots & \vdots & \vdots \end{pmatrix}. \tag{3.46}$$

By comparing modes

$$\boldsymbol{\xi}^t X \frac{d}{dx} D(x)\Big|_{x=0} \boldsymbol{A} + \boldsymbol{\xi}^t X \frac{d}{dx} D(-x)\Big|_{x=0} \boldsymbol{B} = U, \qquad 0 \le y \le h. \tag{3.47}$$

On multiplying (3.47) with $\boldsymbol{\xi}$ and integrating from 0 to a

$$\int_0^a \boldsymbol{\xi}\boldsymbol{\xi}^t dy X \frac{d}{dx} D(x)\Big|_{x=0} \boldsymbol{A} + \int_0^a \boldsymbol{\xi}\boldsymbol{\xi}^t dy X \frac{d}{dx} D(-x)\Big|_{x=0} \boldsymbol{B} = U \int_0^h \boldsymbol{\xi}(y) dy. \tag{3.48}$$

Equation (3.48) can also be written as

$$iX \frac{d}{dx} D(x)\Big|_{x=0} \boldsymbol{A} - iX \frac{d}{dx} D(-x)\Big|_{x=0} \boldsymbol{B} = UQ, \tag{3.49}$$

where

$$Q_m = \int_0^h \boldsymbol{\xi}(y)dy$$
$$= \begin{cases} \frac{h}{\sqrt{a}}, & m = 0, \\ \sqrt{\frac{2}{a}}\frac{a}{m\pi}\left\{\sin(\frac{h\pi}{a})\right\}, & m \geq 1. \end{cases}$$

Therefor (3.49) can also written as

$$XD_0\boldsymbol{A} - XD_0\boldsymbol{B} = -iQU. \tag{3.50}$$

From (3.50) the unknown $\boldsymbol{A}$ can be evaluated as

$$XD_0\boldsymbol{A} = XD_0\boldsymbol{B} - iQU,$$

$$\boldsymbol{A} = \boldsymbol{B} - iD_0^{-1}X^{-1}QU, \tag{3.51}$$

where

$$D_0 = \begin{pmatrix} \eta_0 & 0 & 0 & \dots & 0 & \dots \\ 0 & \eta_1 & 0 & \dots & 0 & \dots \\ \vdots & \vdots & \eta_2 & 0 & 0 & \dots \\ \vdots & \vdots & \vdots & \vdots & \vdots & \vdots \\ 0 & 0 & 0 & \eta_n & 0 & \dots \\ \vdots & \vdots & \vdots & \vdots & \vdots & \vdots \end{pmatrix}. \tag{3.52}$$

3.4 Wave Propagation in Lined Duct Radiated by Plane Piston

We consider the sound propagation in a two dimensional channel, as shown in Fig. 3.2. The lower wall at $y = 0$ is acoustically rigid while the upper wall at $y = a$ is compliant and is describe by a varying admittance $Y(\omega)$. It can be obtain by $Y(\omega) = \frac{1}{Z(\omega)}$, since purely reacting liner is consider here. We can derive the expression of the impedance analytically.

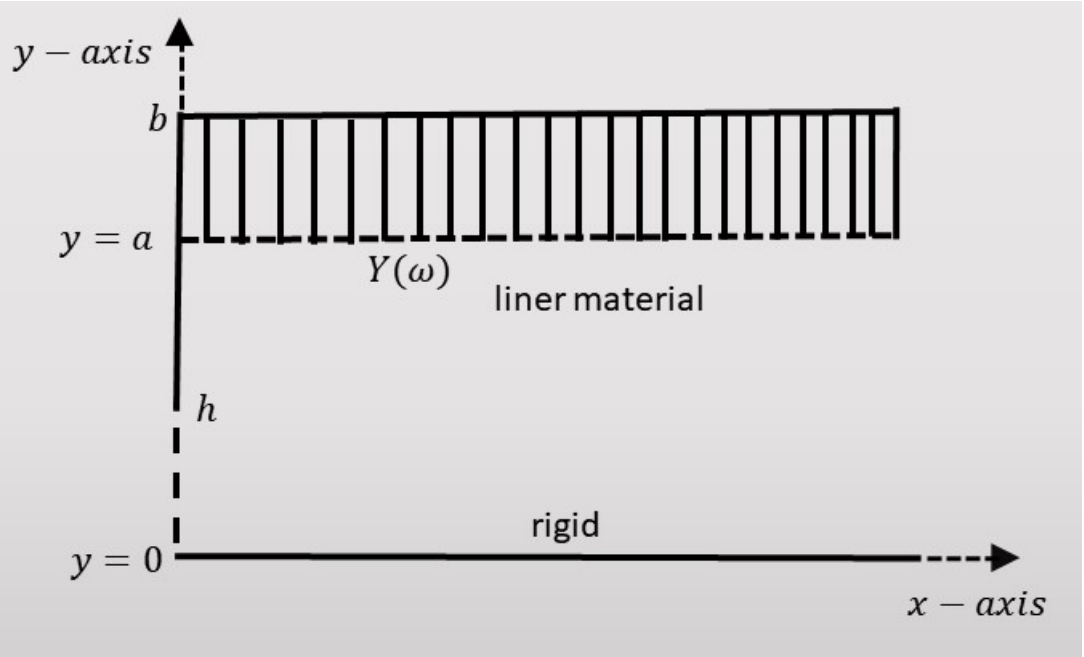

FIGURE 3.2: The physical configuration of duct.

• Liner Condition

In a single lyer between $a \leq y \leq b$, the acoustic pressure satisfies the one dimensional wave equation

$$\frac{\partial^2 \bar{P}}{\partial \bar{y}^2} = \frac{1}{\bar{c}^2} \frac{\partial^2 \bar{p}}{\partial t^2}. \tag{3.53}$$

On using the harmonic time dependence $e^{-i\omega t}$, we can get

$$\frac{\partial p}{\partial y} = -\omega^2 p(y), \tag{3.54}$$

where $\omega = 2\pi f H/c$ is the normalized frequency. The following all quantities are non-dimensionalized length with the waveguide height H. The solution of the (3.54) is

$$p(y) = c_1 \cos(\omega y) + c_2 \sin(\omega y). \tag{3.55}$$

In one dimensional setting (3.5), leads to

$$v = -\frac{i}{\omega} \frac{\partial p}{\partial y}, \tag{3.56}$$

where $v = \boldsymbol{v}.\hat{\boldsymbol{n}}$ is the normal velocity. On using (3.55) into (3.56), we get

$$v = \frac{1}{i\omega}(-c_1\omega\sin(\omega y) + c_2\omega\cos(\omega y)). \tag{3.57}$$

As the upper wall is rigid, the normal velocity yield $v(b) = 0$,

$$\frac{c_1}{c_2} = \frac{1}{\tan(\omega b)}. \tag{3.58}$$

By using (3.55), one may get

$$Z = \frac{p(y)}{v}. \tag{3.59}$$

By substituting (3.55) and (3.57), (3.59) reveals

$$Z(\omega) = i\cot[\omega(b-y)]. \tag{3.60}$$

Thus, the normalized admittance of liner wall at $y = a$, takes the form

$$Y(\omega) = \frac{1}{Z(\omega)}$$

or

$$Y(\omega) = -i\tan[\omega(b-a)]. \tag{3.61}$$

Hence, for liner wall backed by rigid cavity at $y = b$, we can write

$$\frac{\partial p}{\partial y} = i\omega Y(\omega)p(y), \qquad y = a, \tag{3.62}$$

For rigid wall

$$\frac{\partial p}{\partial y} = 0, \qquad y = 0. \tag{3.63}$$

3.5 Multimodal Solution

Consider incident radiation of acoustic waves propagation in duct towards positive x-direction. The travelling waves of guiding channel can be expressed as

$$p(x,y) = \sum_{n=0}^{\infty} A_n \psi_n(y) e^{i\eta_n x}. \tag{3.64}$$

Here the quantity $\psi_n(y)$ determines the shape of n^{th} mode propagating towards positive x-direction having n^{th} mode wavenumber η_n and amplitude A_n. Apparently, these quantities are unknowns. We may determine these unknowns with Multimodal procedure. By using (3.64) into (3.13) and using conditions (3.62)-(3.63), we get

$$\left\{ \frac{d^2}{dy^2} + \gamma_n^2 \right\} \psi_n(y) = 0, \tag{3.65}$$

$$\psi_n'(0) = 0, \tag{3.66}$$

$$\psi_n'(a) = i\omega Y(\omega) \psi(a), \tag{3.67}$$

where $\gamma_n = \sqrt{K^2 - \eta_n^2}$ and prime shows the differentiation with respect to involved variable. To project the solution of differential system (3.65)-(3.67), we formulate the corresponding eigenvalue problem, that is

$$\frac{d^2 \xi_n(y)}{dy^2} + \alpha_n^2 \xi_n(y) = 0, \tag{3.68}$$

$$\xi_n{}'(0) = 0, \tag{3.69}$$

$$\xi_n{}'(a) = 0. \tag{3.70}$$

On solving (3.68) subject to (3.69)-(3.70), we get the orthonormal eigenfunction

$$\xi_n = \Lambda_n \cos(\alpha_n y); \quad n = 0, 1, 2, \cdots \tag{3.71}$$

where $\alpha_n = n\pi/a, \quad n = 0, 1, 2, \cdots$ are the eigenvalues.
Note the orthonormal functions ξ_n satisfy the relation

$$\int_0^a \xi_n(y) \xi_m(y) = \delta_{mn}, \tag{3.72}$$

where δ_{mn} is kronecker delta

$$\delta_{mn} = \begin{cases} 1 & m = n, \\ 0 & m \neq 0. \end{cases}$$

To project the solution of (3.65)-(3.67), we write $\psi_n(y)$ as the linear combination of orthonormal basis functions as:

$$\psi_n(y) = \sum_{m=0}^{\infty} B_{nm}\xi_{nm}(y) = \boldsymbol{\xi}^t \boldsymbol{B}, \tag{3.73}$$

where

$$\boldsymbol{\xi} = \begin{pmatrix} \xi_{n0} \\ \xi_{n1} \\ \vdots \\ \xi_{nm} \\ \vdots \end{pmatrix} \qquad \text{and} \qquad \boldsymbol{B} = \begin{pmatrix} B_{n0} \\ B_{n1} \\ \vdots \\ B_{nm} \\ \vdots \end{pmatrix}. \tag{3.74}$$

Note that superscript t in (3.73) of $\boldsymbol{\xi}$ represent the transpose of vector. On multiplying (3.65) with $\boldsymbol{\xi}$ and integrating over y from 0 to a, we get

$$\int_0^a \boldsymbol{\xi}\frac{d^2\psi_n}{dy^2}dy + \gamma_n^2 \int_0^a \boldsymbol{\xi}\psi_n dy = 0. \tag{3.75}$$

The solution of first integral of (3.75) can be obtained by performing integration by parts as:

$$\int_0^a \boldsymbol{\xi}\frac{d^2\psi_n}{dy^2}dy = \left(\boldsymbol{\xi}(y)\frac{d\psi_n}{dy}\right)\Bigg|_0^a - \left(\frac{d\boldsymbol{\xi}}{dy}\psi_n\right)\Bigg|_0^a + \int_0^a \psi_n \frac{d^2\boldsymbol{\xi}}{dy^2}dy. \tag{3.76}$$

On using boundary conditions (3.66)-(3.67) and (3.69)-(3.70), we get

$$\int_0^a \boldsymbol{\xi}\frac{d^2\psi_n}{dy^2}dy = i\omega Y(\omega)\psi(a)\boldsymbol{\xi} + \int_0^a \psi_n \frac{d^2\boldsymbol{\xi}}{dy^2}dy. \tag{3.77}$$

Therefore (3.75), takes the form

$$i\omega Y(\omega)\psi(a)\boldsymbol{\xi} + \int_0^a \psi_n \frac{d^2\boldsymbol{\xi}}{dy^2}dy + \gamma_n^2 \int_0^a \boldsymbol{\xi}\psi_n dy = 0. \tag{3.78}$$

By substituting (3.71) into (3.78), we obtain

$$i\omega Y(\omega)\psi(a)\xi_n - \int_0^a (\frac{m\pi}{a})^2\psi_n\xi_n dy + \gamma_n^2\int_0^a \xi_n\psi_n dy = 0, \tag{3.79}$$

or

$$i\omega Y(\omega)\psi(a)\xi_n\xi_m - \int_0^a (\frac{m\pi}{a})^2\psi_n\xi_n\xi_m dy + \gamma_n^2\int_0^a \xi_n\xi_m\psi_n dy = 0. \tag{3.80}$$

On using (3.73) into (3.80), we get

$$\begin{aligned} i\omega Y(\omega)\sum_{p=0}^{\infty} B_{np}\xi_{np}\xi_{nm} - (\frac{m\pi}{a})^2\int_0^a \sum_{p=0}^{\infty} B_{np}\xi_{np}\xi_{nm}dy \\ +\gamma_n^2\int_0^a \sum_{p=0}^{\infty} B_{np}\xi_{np}\xi_{nm}dy = 0. \end{aligned} \tag{3.81}$$

By using (3.72), (3.81) leads to

$$i\omega Y(\omega)\sum_{p=0}^{\infty} B_{np}\xi(0)\xi(0) - (\frac{m\pi}{a})^2\sum_{p=0}^{\infty} B_{np}\delta_{pm} + \gamma_n^2\sum_{p=0}^{\infty} B_{np}\delta_{pm} = 0. \tag{3.82}$$

In a matrix form, (3.82) can be written as

$$i\omega Y(\omega).M\boldsymbol{B} - N_1 I\boldsymbol{B} + \gamma_n^2 I\boldsymbol{B} = 0, \tag{3.83}$$

or

$$\gamma_n^2 I\boldsymbol{B} = N_1 I\boldsymbol{B} - i\omega Y(\omega).M\boldsymbol{B}, \tag{3.84}$$

where

$$N_1 = \begin{pmatrix} 0 & 0 & 0 & \dots & 0 \\ 0 & \frac{\pi^2}{a^2} & \vdots & \vdots & \vdots \\ \vdots & \vdots & \vdots & \vdots & \vdots \\ 0 & 0 & 0 & \frac{m^2\pi^2}{a^2} & \vdots \\ \vdots & \vdots & \vdots & \vdots & \vdots \end{pmatrix} \tag{3.85}$$

and $M = \xi_m(0)\xi_n(0)$.

Since $\gamma_n^2 = K^2 - \eta_2^2$, using (3.61) therefore (3.84) can be written as

$$\eta_n^2 I\boldsymbol{B} = [K^2 I + \omega\tan(\omega(b-a))M - N_1]\boldsymbol{B}. \tag{3.86}$$

By computing the matrix eigenvalue problem for a value of ω we can get the eigenvalue and eigenvector the wavenumber are calculated by η_n^2. A purely reacting liner is considered here so the wavenumber is may real and imaginary values.
Being aware of eigenvalues and eigenvectors the resulting field potential in duct can be written as:

$$p(x,y) = \boldsymbol{\xi}^t[XD(x)\boldsymbol{A} + XD(-x)\boldsymbol{B}], \tag{3.87}$$

where

$$D(x) = \begin{pmatrix} e^{i\eta_0 x} & 0 & 0 & \dots & 0 & \dots \\ 0 & e^{i\eta_1 x} & 0 & \dots & 0 & \dots \\ \vdots & \vdots & e^{i\eta_2 x} & 0 & 0 & \dots \\ \vdots & \vdots & \vdots & \vdots & \vdots & \vdots \\ 0 & 0 & 0 & e^{i\eta_n x} & 0 & \dots \\ \vdots & \vdots & \vdots & \vdots & \vdots & \vdots \end{pmatrix}, \tag{3.88}$$

$$\boldsymbol{A}^t = \begin{bmatrix} A_0 & A_1 & \dots & A_n & \dots \end{bmatrix} \tag{3.89}$$

and

$$\boldsymbol{B}^t = \begin{bmatrix} \delta_{00} & \delta_{10} & \dots & \delta_{n0} & \dots \end{bmatrix}. \tag{3.90}$$

On differentiating (3.87) with respect to x, we find

$$\frac{\partial p}{\partial x} = \boldsymbol{\xi}^t[X\frac{d}{dx}D(x)\boldsymbol{A} + X\frac{d}{dx}D(-x)\boldsymbol{B}], \tag{3.91}$$

where

$$\frac{d}{dx}D(x)\bigg|_{x=0} = \begin{pmatrix} i\eta_0 e^{i\eta_0 x} & 0 & 0 & \dots & 0 & \dots \\ 0 & i\eta_1 e^{i\eta_1 x} & 0 & \dots & 0 & \dots \\ \vdots & \vdots & i\eta_2 e^{i\eta_2 x} & 0 & 0 & \dots \\ \vdots & \vdots & \vdots & \vdots & \vdots & \vdots \\ 0 & 0 & 0 & i\eta_n e^{\eta_n x} & 0 & \dots \\ \vdots & \vdots & \vdots & \vdots & \vdots & \vdots \end{pmatrix}. \tag{3.92}$$

By comparing modes

$$\boldsymbol{\xi}^t X \frac{d}{dx} D(x)\Big|_{x=0} \boldsymbol{A} + \boldsymbol{\xi}^t X \frac{d}{dx} D(-x)\Big|_{x=0} \boldsymbol{B} = U, \qquad 0 \le y \le h. \tag{3.93}$$

On multiplying (3.93) with $\boldsymbol{\xi}$ and integrating from 0 to a

$$\int_0^a \boldsymbol{\xi}\boldsymbol{\xi}^t dy X \frac{d}{dx} D(x)\Big|_{x=0} \boldsymbol{A} + \int_0^a \boldsymbol{\xi}\boldsymbol{\xi}^t dy X \frac{d}{dx} D(-x)\Big|_{x=0} \boldsymbol{B} = U \int_0^h \boldsymbol{\xi}(y) dy, \tag{3.94}$$

or

$$iX \frac{d}{dx} D(x)\Big|_{x=0} \boldsymbol{A} - iX \frac{d}{dx} D(-x)\Big|_{x=0} \boldsymbol{B} = UQ, \tag{3.95}$$

where

$$\begin{aligned} Q_m &= \int_0^h \boldsymbol{\xi}(y) dy, \\ &= \begin{cases} \frac{h}{\sqrt{a}}, & m = 0, \\ \sqrt{\frac{2}{a}} \frac{a}{m\pi} \left\{ \sin(\frac{h\pi}{a}) \right\}, & m \ge 1. \end{cases} \end{aligned}$$

Equation (3.95) can also written as

$$XD_0\boldsymbol{A} - XD_0\boldsymbol{B} = QU. \tag{3.96}$$

From (3.96), the unknown $\boldsymbol{A}$ can be evaluated as:

$$\boldsymbol{A} = \boldsymbol{B} - iD_0^{-1}X^{-1}QU. \tag{3.97}$$

where

$$D_0 = \begin{pmatrix} \eta_0 & 0 & 0 & \dots & 0 & \dots \\ 0 & \eta_1 & 0 & \dots & 0 & \dots \\ \vdots & \vdots & \eta_2 & 0 & 0 & \dots \\ \vdots & \vdots & \vdots & \vdots & \vdots & \vdots \\ 0 & 0 & 0 & \eta_n & 0 & \dots \\ \vdots & \vdots & \vdots & \vdots & \vdots & \vdots \end{pmatrix}. \tag{3.98}$$

3.6 Numerical Results

Here the numerical results are displayed. The model problems have excitation from the plane piston moving with constant velocity U. The duct contain reacting lining along $a \leq y \leq b$. For computational results the values of dimensionless heights are considered as $H = 3$, $a = 25/3$ and $b = 30/3$, where the speed of sound is taken 343.5m/s.

3.6.1 Scattering Amplitudes in Rigid Duct

In Figs. 3.3 and 3.4, the movement of wavenumber of mode 0, mode 1 and mode 2 are shown against frequency ω. The real part of these modes are shown in Fig. 3.3 while imaginary parts are displayed in Fig. 3.4. The trajectory of these modes have impact on the wave propagation whose absolute amplitudes are depicted in Figs. 3.5-3.7.

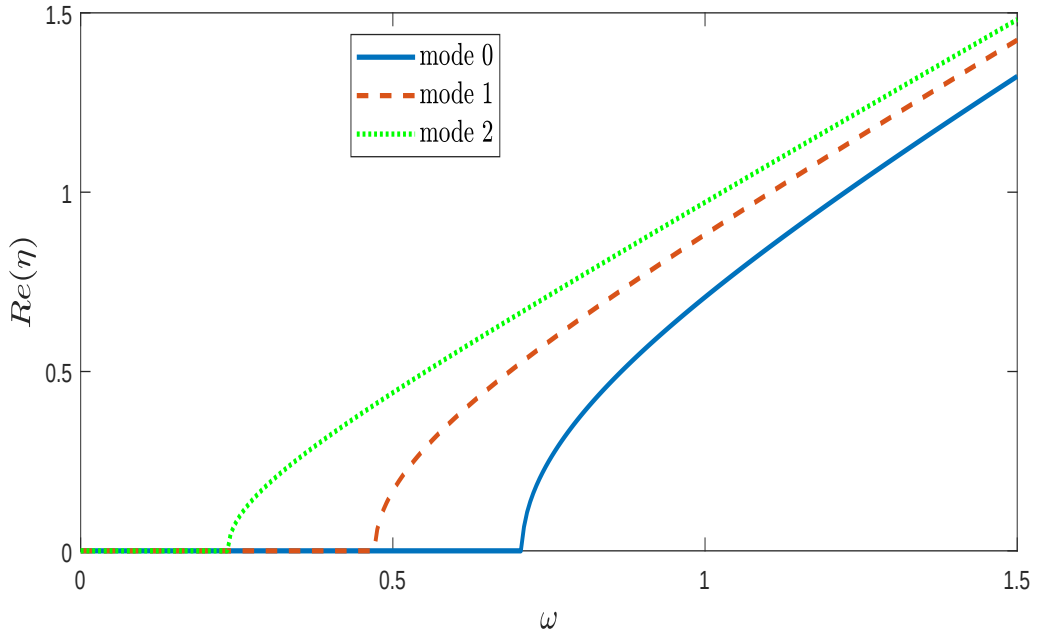

FIGURE 3.3: Trajectories of the real parts of η as a function of frequency ω.

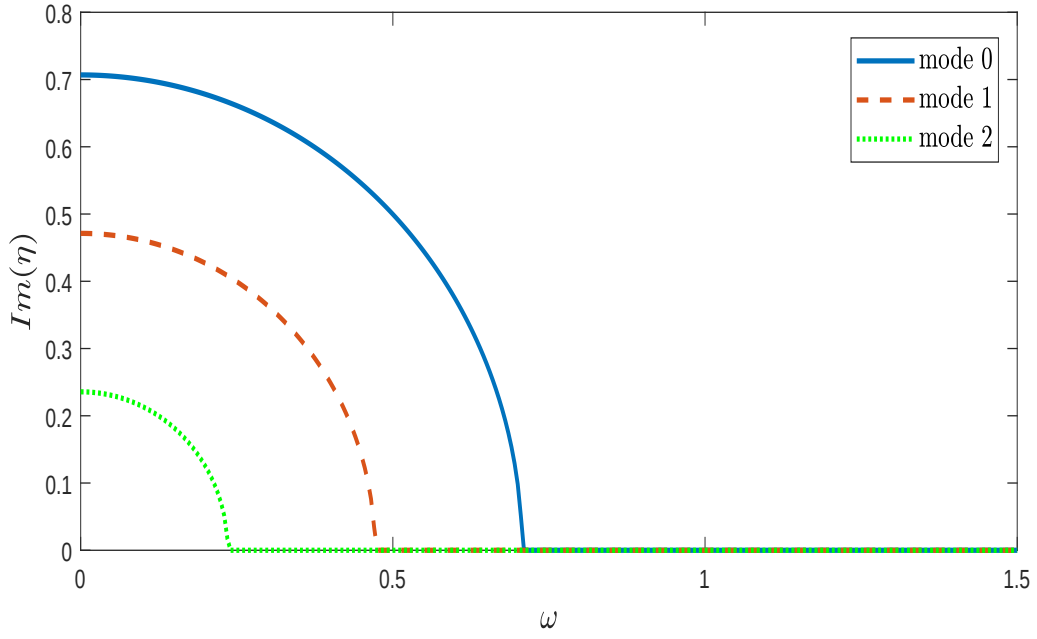

FIGURE 3.4: Trajectories of the real parts of η as a function of frequency ω.

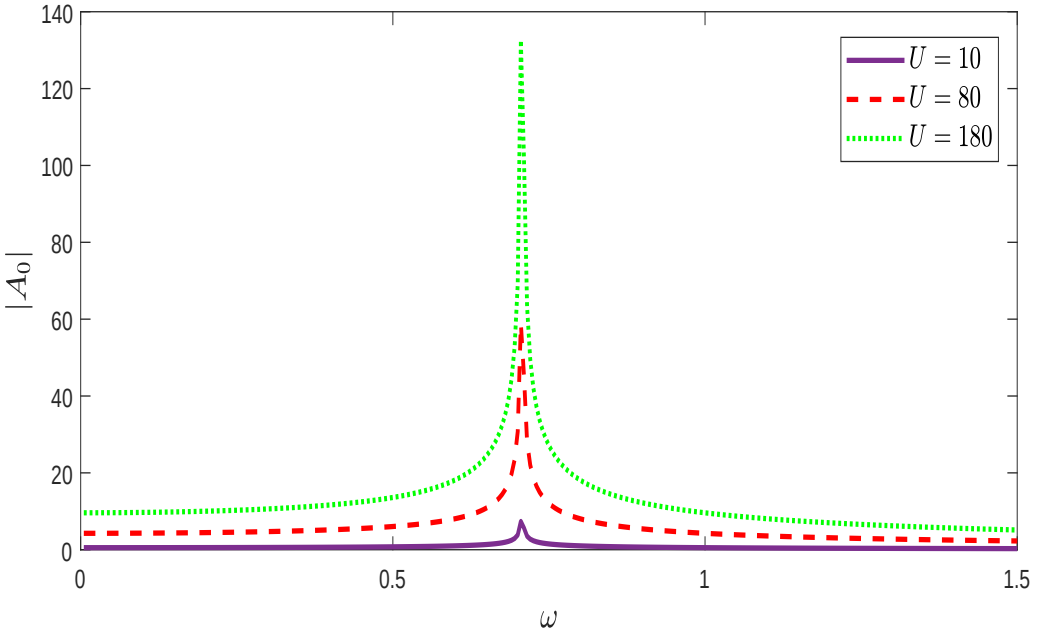

FIGURE 3.5: The absolute value of fundamental mode amplitude $|A_0|$ against frequency ω.

In Fig. 3.5, the absolute value of fundamental amplitude is ploted shown against frequency. For different values of piston velocity U. It can be seen that by changing the velocity of the piston the magnitude of amplitude is varied.

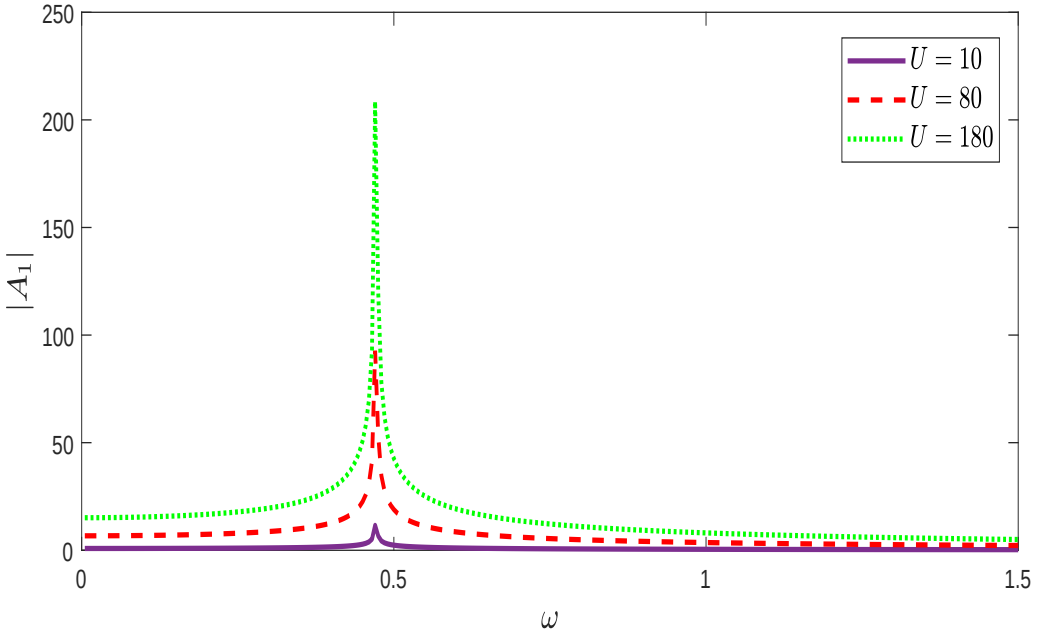

FIGURE 3.6: The absolute value of fundamental mode amplitude $|A_1|$ against frequency ω.

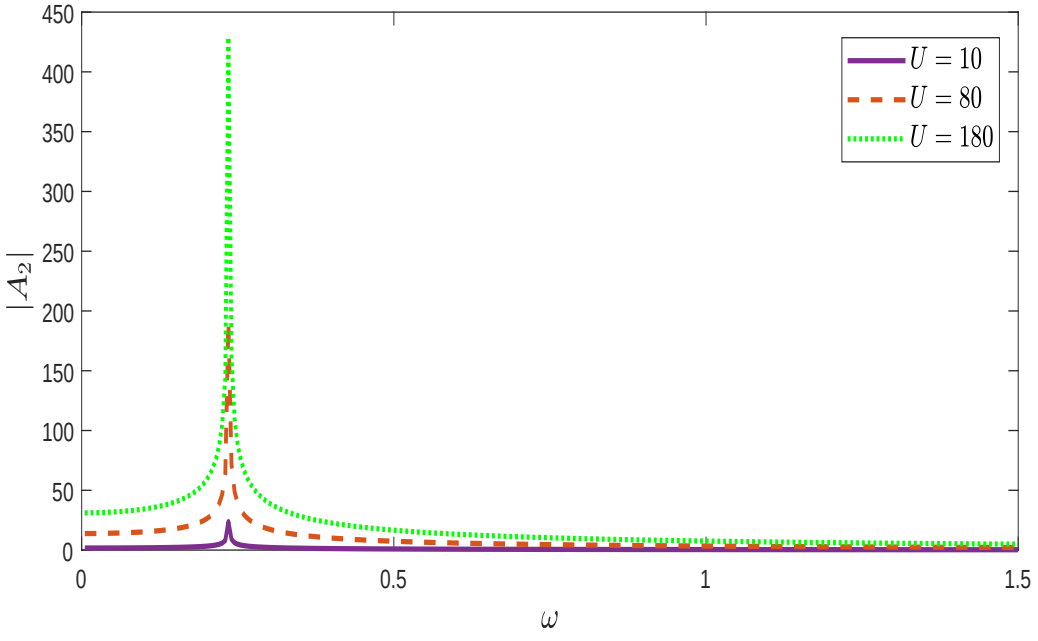

FIGURE 3.7: The absolute value of fundamental mode amplitude $|A_2|$ against frequency ω.

In Figs. 3.6 and 3.7, the absolute values of secondary mode amplitude $|A_1|$ and third mode amplitude $|A_2|$ are respectively shown. These modes are produced by

plane piston of velocity U taken as 10m/s, 80m/s and 180m/s. It can be clearly seen from Figs. 3.6- 3.7, the absolute values of $|A_0|$, $|A_1|$ and $|A_2|$ are increasing by increasing the velocity of the plane piston U.

3.6.2 Scattering Amplitudes in Lined Duct

In Figs. 3.8 and 3.9, the movement of wavenumber of mode 0, mode 1 and mode 2 are shown against frequency ω. The real part of these modes are shown in Fig. 3.8 while imaginary parts are displayed in Fig. 3.9. The trajectory of these modes have impact on the wave propagation whose absolute amplitudes are depicted in Figs. 3.10-3.12. In Fig. 3.10, the absolute value of fundamental amplitude is ploted shown against frequency. For different values of piston velocity U. It can be seen that by changing the velocity of the piston the magnitude of amplitude is varied. However, in all the figures the spikes occured in curves are because of the variation of eigenvalues. The trajectories of modes wavenumber η is evident of this fact. (see Figs. 3.8-3.9).

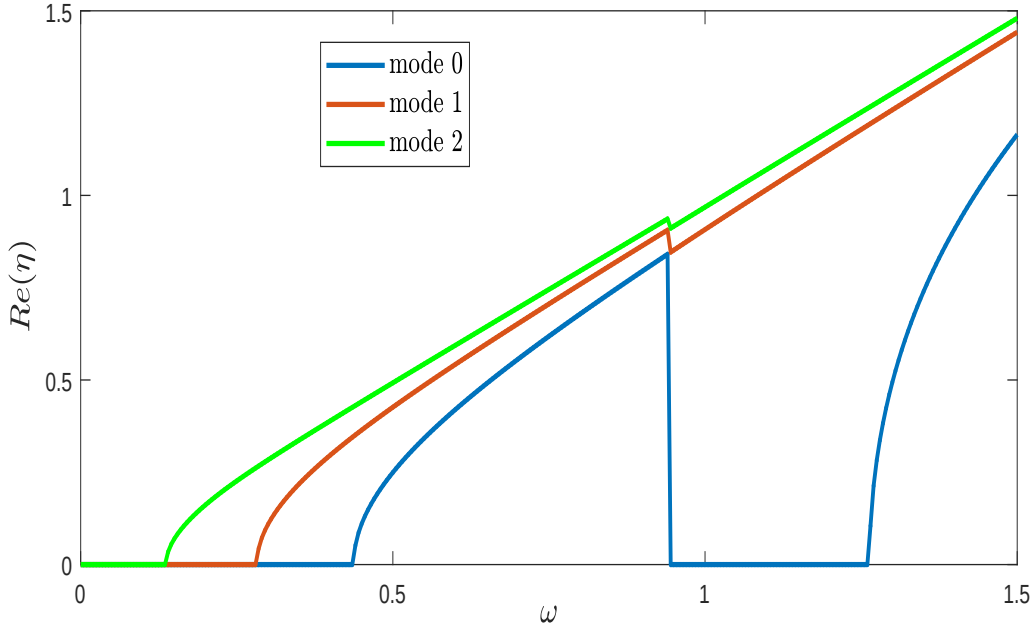

FIGURE 3.8: Trajectories of the real parts of η as a function of frequency ω.

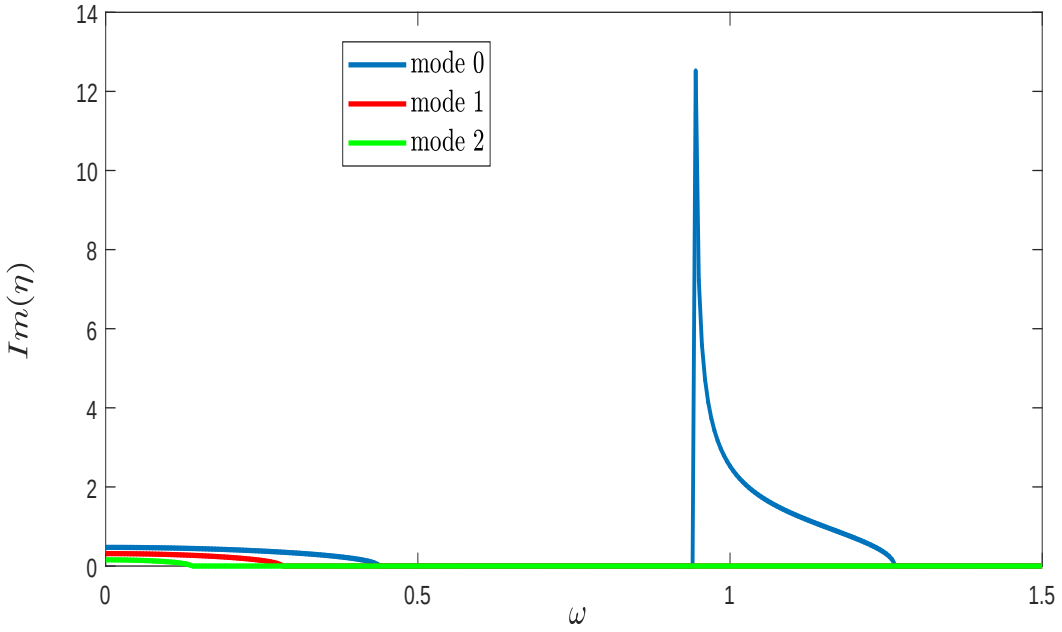

FIGURE 3.9: Trajectories of the imaginary parts of η as a function of frequency ω.

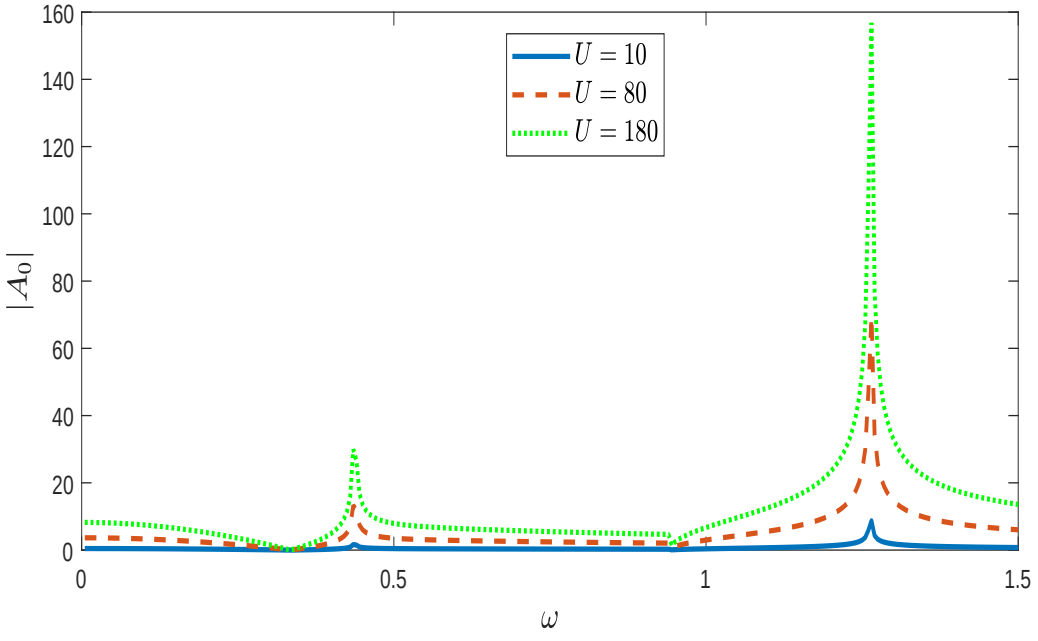

FIGURE 3.10: The absolute value of fundamental mode amplitude $|A_0|$ against frequency ω.

In Figs. 3.11 and 3.12, the absolute values of secondary mode amplitude $|A_1|$ and third mode amplitude $|A_2|$ are respectively shown. These modes are produced by

plane piston of velocity U taken as 10m/s, 80m/s and 180m/s. It can be clearly seen from Figs. 3.10- 3.12, the absolute values of $|A_0|$, $|A_1|$ and $|A_2|$ are increasing by increasing the velocity of the plane piston U.

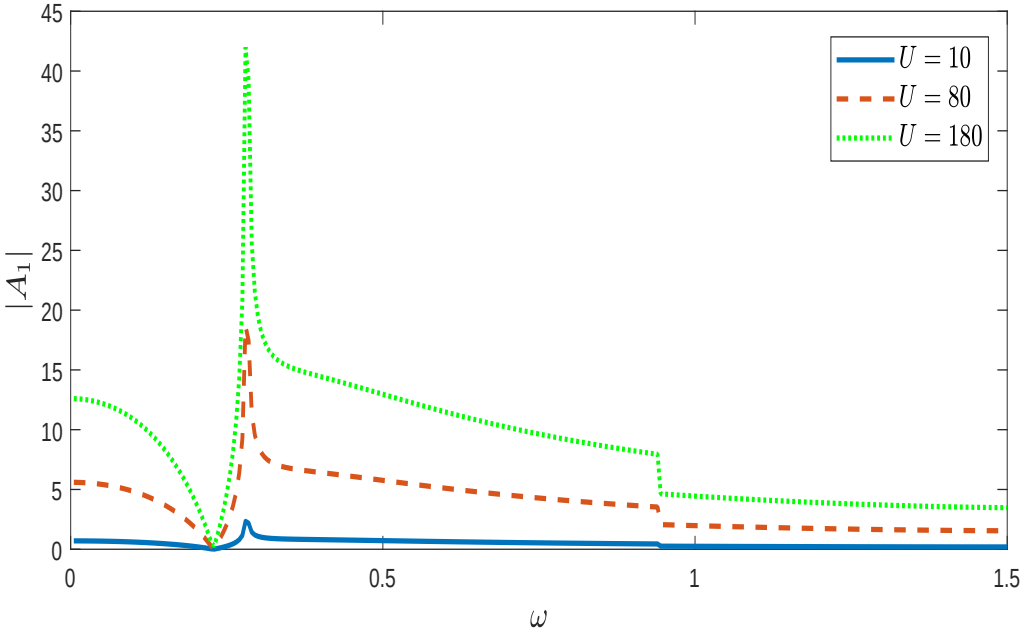

FIGURE 3.11: The absolute value of secondary mode amplitude $|A_1|$ against frequency ω.

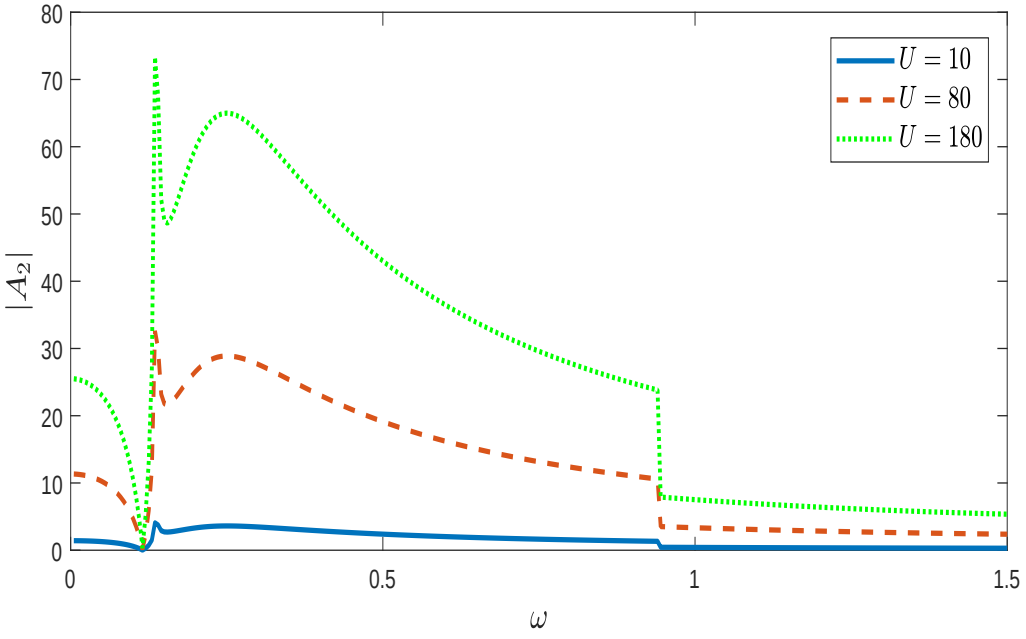

FIGURE 3.12: The absolute value of third mode amplitude $|A_2|$ against frequency ω.

Chapter 4

Acoustic Propagation and Scattering through the Lined Cavities

In this chapter, we discuss two waveguide problems liners inclusion. The first problem comprises acoustic liners in a single cavity whilst the second problem include double lined cavities. The propagation and attenuation through these cavities are discussed by using Multimodal technique. Section 4.1 contains the mathematical modelling of single lined cavities. The solution of the governing problems is found in Section 4.2. In Section 4.3, the modelling of double lined cavities is discussed while its solution is explained in Section 4.4. The computational results and discussion is provided in Section 4.5.

4.1 Scattering through Single Lined Cavity

Consider an acoustic plane wave propagating form negative x-direction towards $x = 0$, in an infinite waveguide. At $x = a$, it will spread into different directions of infinite reflected and transmitted modes. The waveguide is divided into three regions. First inlet; having incident and reflected fields and third outlet; which

contains outgoing field, whereas the second region is lined through locally reacting liners where in attenuation take place. The inside of the waveguide is filled with compressible fluid of density ρ and sound speed c. The physical configuration of the waveguide is shown in Fig. 4.1.

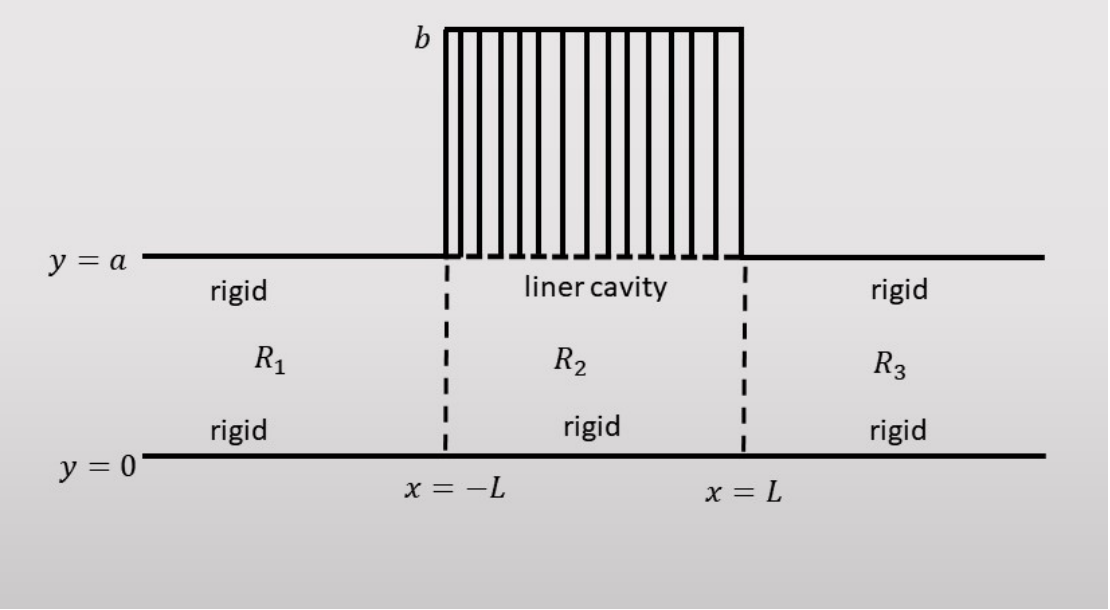

FIGURE 4.1: The physical configuration of waveguide.

The dimensionless pressure in duct regions can be written as

$$p(x,y) = \begin{cases} p_1(x,y), & x \le -L, \quad 0 \le y \le a, \\ p_2(x,y), & -L \le x \le L, \quad 0 \le y \le b, \\ p_3(x,y), & x \ge L, \quad 0 \le y \le a. \end{cases} \tag{4.1}$$

The dimensional form of boundary conditions can be written as

$$\frac{\partial p_1}{\partial y} = 0, \qquad y = 0,\ a \qquad x \le -L, \tag{4.2}$$

$$\frac{\partial p_2}{\partial y} = 0, \qquad y = 0, \qquad -L \le x \le L, \tag{4.3}$$

$$\frac{\partial p_2}{\partial y} = i\omega Y(\omega) p_2(y), \qquad y = a, [70] \quad -L \le x \le L, \tag{4.4}$$

$$\frac{\partial p_3}{\partial y} = 0, \qquad y = 0,\ a \qquad x \ge L. \tag{4.5}$$

In next section the Multimodal solution of the problem is explained.

4.2 Multimodal Solution

To determined the eigenmodes of central region R_2 analyzed the acoustic scattering in expansion chamber having liner cavities, we use Multimodal technique, for this we assume insatz

$$p(x,y) = \sum_{n=0}^{\infty} A_n \psi_n(y) e^{i\eta_n x}. \tag{4.6}$$

By using (4.6) into (3.13) and using boundary conditions (4.3) and (4.4), we get

$$\left\{ \frac{d^2}{dy^2} + \gamma_n^2 \right\} \psi_n(y) = 0, \tag{4.7}$$

$$\psi_n'(0) = 0, \tag{4.8}$$

$$\psi_n{}'(a) = i\omega Y(\omega)\psi(a), \tag{4.9}$$

where $\gamma_n = \sqrt{K^2 - \eta_n^2}$ and prime shows the differentiation with respect to involved variable. To project the solution of differential system (4.7)-(4.9), we formulate the corresponding eigenvalue problem, that is

$$\frac{d^2\xi_n(y)}{dy^2} + \alpha_n^2 \xi_n(y) = 0, \tag{4.10}$$

$$\xi_n{}'(0) = 0, \tag{4.11}$$

$$\xi_n{}'(a) = 0. \tag{4.12}$$

On solving (4.10) subject to (4.11)-(4.12), we get the orthonormal eigenfunction as:

$$\xi_n = \Lambda_n \cos(\alpha_n y); \quad n = 0, 1, 2, \cdots \tag{4.13}$$

where $\alpha_n = n\pi/a, \quad n = 0, 1, 2, \cdots$ are the eigenvalues.

Note the orthonormal functions ξ_n satisfy the relation

$$\int_0^a \xi_n(y)\xi_m(y) = \delta_{mn}, \tag{4.14}$$

where δ_{mn} is kronecker delta

$$\delta_{mn} = \begin{cases} 1, & m = n, \\ 0, & m \neq 0. \end{cases}$$

To project the solution of (4.7)-(4.9), we write $\psi_n(y)$ as the linear combination of orthonormal basis functions as:

$$\psi_n(y) = \sum_{n=0}^{\infty} B_{nm}\xi_{nm}(y) = \boldsymbol{\xi}^t \boldsymbol{B}, \tag{4.15}$$

where

$$\boldsymbol{\xi} = \begin{pmatrix} \xi_{n0} \\ \xi_{n1} \\ \vdots \\ \xi_{nm} \\ \vdots \end{pmatrix} \quad \text{and} \quad \boldsymbol{B} = \begin{pmatrix} B_{n0} \\ B_{n1} \\ \vdots \\ B_{nm} \\ \vdots \end{pmatrix}. \tag{4.16}$$

Note that superscript t in (4.15) of $\boldsymbol{\xi}$ represent the transpose of vector. On multiplying (4.7) with $\boldsymbol{\xi}$ and integrating over y from 0 to a, we get

$$\int_0^a \boldsymbol{\xi}\frac{d^2\psi_n}{dy^2}dy + \gamma_n^2 \int_0^a \boldsymbol{\xi}\psi_n dy = 0. \tag{4.17}$$

The solution of first integral of (4.17) can be obtained by performing integration by parts as:

$$\int_0^a \boldsymbol{\xi}\frac{d^2\psi_n}{dy^2}dy = \left(\boldsymbol{\xi}(y)\frac{d\psi_n}{dy}\right)\Bigg|_0^a - \left(\frac{d\boldsymbol{\xi}}{dy}\psi_n\right)\Bigg|_0^a + \int_0^a \psi_n\frac{d^2\boldsymbol{\xi}}{dy^2}dy. \tag{4.18}$$

On using boundary conditions (4.8)-(4.9) and (4.11)-(4.12), we get

$$\int_0^a \boldsymbol{\xi}\frac{d^2\psi_n}{dy^2}dy = i\omega Y(\omega)\psi(a)\boldsymbol{\xi} + \int_0^a \psi_n\frac{d^2\boldsymbol{\xi}}{dy^2}dy. \tag{4.19}$$

Therefore (4.17), takes the form

$$i\omega Y(\omega)\psi(a)\boldsymbol{\xi} + \int_0^a \psi_n\frac{d^2\boldsymbol{\xi}}{dy^2}dy + \gamma_n^2 \int_0^a \boldsymbol{\xi}\psi_n dy = 0. \tag{4.20}$$

On using (4.13) into (4.20), we find

$$i\omega Y(\omega)\psi(a)\boldsymbol{\xi} - \int_0^a (\frac{m\pi}{a})^2 \boldsymbol{\xi}\psi_n dy + \gamma_n^2 \int_0^a \boldsymbol{\xi}\psi_n dy = 0, \tag{4.21}$$

or

$$i\omega Y(\omega)\psi(a)\boldsymbol{\xi} - \int_0^a (\frac{m\pi}{a})^2 \xi_n\xi_m\psi_n dy + \gamma_n^2 \int_0^a \xi_n\xi_m\psi_n dy = 0. \tag{4.22}$$

By invoking (4.15) into (4.22), we find

$$\begin{aligned} i\omega Y(\omega)\sum_{p=0}^{\infty} B_{np}\xi_{np}\xi_{nm} - \int_0^a \sum_{p=0}^{\infty} (\frac{m\pi}{a})^2 B_{np}\xi_{np}\xi_{nm}dy \\ +\gamma_n^2 \int_0^a \sum_{p=0}^{\infty} B_{np}\xi_{np}\xi_{nm}dy = 0. \end{aligned} \tag{4.23}$$

By using (4.14), (4.23) leads to

$$i\omega Y(\omega)\sum_{p=0}^{\infty} B_{np}\xi(0)\xi(0) - (\frac{m\pi}{a})^2 \sum_{p=0}^{\infty} B_{np}\delta_{pm} + \gamma_n^2 \sum_{p=0}^{\infty} B_{np}\delta_{pm} = 0. \tag{4.24}$$

In a matrix form, (4.24) can be written as

$$i\omega Y(\omega).M\boldsymbol{B} - N_1 I\boldsymbol{B} + \gamma_n^2 I\boldsymbol{B} = 0, \tag{4.25}$$

or

$$\gamma_n^2 I\boldsymbol{B} = N_1 I\boldsymbol{B} - i\omega Y(\omega).M\boldsymbol{B}, \tag{4.26}$$

where

$$N_1 = \begin{pmatrix} 0 & 0 & 0 & \dots & 0 \\ 0 & \frac{\pi^2}{a^2} & \vdots & \vdots & \vdots \\ \vdots & \vdots & \vdots & \vdots & \vdots \\ 0 & 0 & 0 & \frac{m^2\pi^2}{a^2} & \vdots \\ \vdots & \vdots & \vdots & \vdots & \vdots \end{pmatrix} \tag{4.27}$$

and $M = \xi_m(0)\xi_n(0)$.

Since $\gamma_n^2 = K^2 - \eta_n^2$ and using (3.61) into (4.26), we find

$$\eta_n^2 I\boldsymbol{B} = [K^2 I + \omega\tan(\omega(b-a))M - N_1]\boldsymbol{B}. \tag{4.28}$$

The pressures in duct regions as liner combination of transverse modes, we may write

$$p_1(x,y) = \sum_{n=0}^{\infty} A_{1n}\psi_n(y)e^{is_n(x+L)} + \sum_{n=0}^{\infty} B_{1n}\psi_n(y)e^{-is_n(x+L)}, \tag{4.29}$$

$$p_2(x,y) = \sum_{n=0}^{\infty} A_{2n}\psi_n(y)e^{i\eta_n x} + \sum_{n=0}^{\infty} B_{2n}\psi_n(y)e^{-i\eta_n x}, \tag{4.30}$$

$$p_3(x,y) = \sum_{n=0}^{\infty} A_{3n}\psi_n(y)e^{is_n(x-L)} + \sum_{n=0}^{\infty} B_{3n}\psi_n(y)e^{-is_n(x-L)}. \tag{4.31}$$

Above equations in matrix form can be written as

$$\boldsymbol{p}_1 = \boldsymbol{\psi}^t[D_1(x+L)\boldsymbol{A}_1 + D_1(-x-L)\boldsymbol{B}_1], \tag{4.32}$$

$$\boldsymbol{p}_2 = \boldsymbol{\psi}^t X[D_2(x)\boldsymbol{A}_2 + D_2(-x)\boldsymbol{B}_2], \tag{4.33}$$

$$\boldsymbol{p}_3 = \boldsymbol{\psi}^t[D_1(x-L)\boldsymbol{A}_3 + D_1(-x+L)\boldsymbol{B}_3]. \tag{4.34}$$

Note that $\{\boldsymbol{A}_1, \boldsymbol{A}_2, \boldsymbol{A}_3\}$ and $\{\boldsymbol{B}_1, \boldsymbol{B}_2, \boldsymbol{B}_3\}$ are unknowns, where $D_2(x)$ is the diagonal matrix with element $e^{i\eta_n(x)}$ and $D_1(x)$ containing the element $e^{is_n(x)}$, where $s_n = \sqrt{K^2 - \alpha_n^2}$ are the axial wavenumber of the rigid walls bounded regions

$$D_1(x) = \begin{pmatrix} e^{is_0x} & 0 & 0 & \dots & 0 & \dots \\ 0 & e^{is_1x} & 0 & \dots & 0 & \dots \\ \vdots & \vdots & e^{is_2x} & 0 & 0 & \dots \\ \vdots & \vdots & \vdots & \vdots & \vdots & \vdots \\ 0 & 0 & 0 & e^{is_nx} & 0 & \dots \\ \vdots & \vdots & \vdots & \vdots & \vdots & \vdots \end{pmatrix} \tag{4.35}$$

and

$$D_2(x) = \begin{pmatrix} e^{i\eta_0x} & 0 & 0 & \dots & 0 & \dots \\ 0 & e^{i\eta_1x} & 0 & \dots & 0 & \dots \\ \vdots & \vdots & e^{i\eta_2x} & 0 & 0 & \dots \\ \vdots & \vdots & \vdots & \vdots & \vdots & \vdots \\ 0 & 0 & 0 & e^{i\eta_nx} & 0 & \dots \\ \vdots & \vdots & \vdots & \vdots & \vdots & \vdots \end{pmatrix}. \tag{4.36}$$

We calculate the unknowns through matching the pressures and normal velocities at interfaces $x = -L$ and $x = L$. Therefore, the continuity of pressures at $x = -L$ and $x = L$ take formulation

$$p_1(-L, y) = p_2(-L, y) \qquad 0 \leq y \leq b, \tag{4.37}$$

and

$$p_2(L, y) = p_3(L, y), \qquad 0 \leq y \leq b, \tag{4.38}$$

respectively. The continuity of normal velocities at $x = -L$ and $x = L$ can be given as

$$\frac{\partial p_1}{\partial x}(-L, y) = \frac{\partial p_2}{\partial x}(-L, y) \qquad 0 \leq y \leq b, \tag{4.39}$$

and

$$\frac{\partial p_2}{\partial x}(L, y) = \frac{\partial p_3}{\partial x}(L, y), \qquad 0 \leq y \leq b. \tag{4.40}$$

Now by using (4.32)-(4.34) into (4.37)-(4.40), one may get

$$\boldsymbol{\psi}^t \left[D_1(0)\boldsymbol{A}_1 + D_1(0)\boldsymbol{B}_1\right] = \boldsymbol{\psi}^t X \left[D_2(-L)\boldsymbol{A}_2 + D_2(L)\boldsymbol{B}_2\right], \tag{4.41}$$

$$\boldsymbol{\psi}^t X \left[D_2(L)\boldsymbol{A}_2 + D_2(-L)\boldsymbol{B}_2\right] = \boldsymbol{\psi}^t \left[D_1(0)\boldsymbol{A}_3 + D_1(0)\boldsymbol{B}_3\right], \tag{4.42}$$

$$\boldsymbol{\psi}^t K_R \left[D_1(0)\boldsymbol{A}_1 - D_1(0)\boldsymbol{B}_1\right] = \boldsymbol{\psi}^t X K_Y \left[D_2(-L)\boldsymbol{A}_2 - D_2(L)\boldsymbol{B}_2\right], \tag{4.43}$$

$$\boldsymbol{\psi}^t X K_Y \left[D_2(L)\boldsymbol{A}_2 - D_2(-L)\boldsymbol{B}_2\right] = \boldsymbol{\psi}^t K_R \left[D_1(0)\boldsymbol{A}_3 - D_1(0)\boldsymbol{B}_3\right]. \tag{4.44}$$

Multiplying (4.41)-(4.44) with $\boldsymbol{\psi}$, integrating over $y = 0$ to $y = a$, then simplifying the following equations:

$$\boldsymbol{A}_1 + \boldsymbol{B}_1 = X[D_2(-L)\boldsymbol{A}_2 + D_2(L)\boldsymbol{B}_2], \tag{4.45}$$

$$K_R(\boldsymbol{A}_1 - \boldsymbol{B}_1) = X K_Y[D_2(-L)\boldsymbol{A}_2 - D_2(L)\boldsymbol{B}_2], \tag{4.46}$$

$$\boldsymbol{A}_3 + \boldsymbol{B}_3 = X[D_2(L)\boldsymbol{A}_2 + D_2(-L)\boldsymbol{B}_2], \tag{4.47}$$

$$K_R(\boldsymbol{A}_3 - \boldsymbol{B}_3) = XK_Y[D_2(L)\boldsymbol{A}_2 - D_2(-L)\boldsymbol{B}_2], \tag{4.48}$$

where K_R and K_Y are diagonal matrices containing the elements of axial wavenumber

$$K_R = \begin{pmatrix} s_0 & 0 & 0 & \dots & 0 & \dots \\ 0 & s_1 & 0 & \dots & 0 & \dots \\ \vdots & \vdots & s_2 & 0 & 0 & \dots \\ \vdots & \vdots & \vdots & \vdots & \vdots & \vdots \\ 0 & 0 & 0 & s_n & 0 & \dots \\ \vdots & \vdots & \vdots & \vdots & \vdots & \vdots \end{pmatrix} \tag{4.49}$$

and

$$K_Y = \begin{pmatrix} \eta_0 & 0 & 0 & \dots & 0 & \dots \\ 0 & \eta_1 & 0 & \dots & 0 & \dots \\ \vdots & \vdots & \eta_2 & 0 & 0 & \dots \\ \vdots & \vdots & \vdots & \vdots & \vdots & \vdots \\ 0 & 0 & 0 & \eta_n & 0 & \dots \\ \vdots & \vdots & \vdots & \vdots & \vdots & \vdots \end{pmatrix}. \tag{4.50}$$

Considering $\boldsymbol{B}_3 = 0$ and then comparing (4.47) with (4.48), it is straight forward to write

$$X[D_2(L)\boldsymbol{A}_2 + D_2(-L)\boldsymbol{B}_2] = K_R^{-1}XK_Y[D_2(L)\boldsymbol{A}_2 - D_2(-L)\boldsymbol{B}_2]. \tag{4.51}$$

Let we define

$$F = X + K_R^{-1}XK_Y \tag{4.52}$$

and

$$G = X - K_R^{-1}XK_Y, \tag{4.53}$$

then (4.51) becomes

$$\boldsymbol{B}_2 = -F^{-1}D_2^{-1}(-L)GD_2(L)\boldsymbol{A}_2. \tag{4.54}$$

By adding (4.47) and (4.48), we get

$$2\boldsymbol{A}_3 = FD_2(L)\boldsymbol{A}_2 + GD_2(-L)\boldsymbol{B}_2. \tag{4.55}$$

But on using the value of $\boldsymbol{B}_2$ from (4.54), (4.55) leads to

$$2\boldsymbol{A}_3 = (FD_2(L) - F^{-1}D_2^{-1}(-L)GD_2(L)GD_2(-L))\boldsymbol{A}_2. \tag{4.56}$$

Now by adding (4.45) and (4.46), it is straight forward to find

$$2\boldsymbol{A}_1 = FD_2(-L)\boldsymbol{A}_2 + GD_2(L)\boldsymbol{B}_2, \tag{4.57}$$

which on using the value of $\boldsymbol{B}_2$ from (4.54) gives

$$2\boldsymbol{A}_1 = (FD_2(-L) - F^{-1}D_2^{-1}(-L)GD_2(L)GD_2(L))\boldsymbol{A}_2. \tag{4.58}$$

By subtracting (4.46) from (4.45), we achieve

$$2\boldsymbol{B}_1 = (GD_2(-L) - F^{-1}D_2^{-1}(-L)GD_2(L)FD_2(L))\boldsymbol{A}_2. \tag{4.59}$$

According to [70] the reflection and transmission coefficients can be written as

$$\boldsymbol{T(t)} = \frac{\boldsymbol{A}_3}{\boldsymbol{A}_1} \tag{4.60}$$

and

$$\boldsymbol{R(r)} = \frac{\boldsymbol{B}_1}{\boldsymbol{A}_1}. \tag{4.61}$$

By using the values of $\boldsymbol{A}_3$ and $\boldsymbol{A}_1$ the transmission coefficient becomes

$$\begin{aligned}\boldsymbol{T(t)} = &(FD_2(L) - F^{-1}D_2^{-1}(-L)GD_2(L)GD_2(-L))\\ &(FD_2(-L) - F^{-1}D_2^{-1}(-L)GD_2(L)GD_2(L))^{-1}.\end{aligned} \tag{4.62}$$

Likewise on using the value of $\boldsymbol{B}_1$ and $\boldsymbol{A}_1$, we achieve the reflection coefficient as

$$\begin{aligned}\boldsymbol{R(r)} = (GD_2(-L) - F^{-1}D_2^{-1}(-L)GD_2(L)FD_2(L))\\ (FD_2(-L) - F^{-1}D_2^{-1}(-L)GD_2(L)GD_2(L))^{-1}.\end{aligned} \tag{4.63}$$

4.3 Scattering through Double Lined Cavities

This Section contains double cavities of acoustic liners. The regions of the waveguide can be termed as R_1, R_2, R_3, R_4 and R_5. The physical configuration is as shown in Fig. 4.2. The regions R_1, R_3, and R_5 are bounded with rigid walls while the regions R_2 and R_4 are bounded below with rigid walls and above with liner cavity walls.

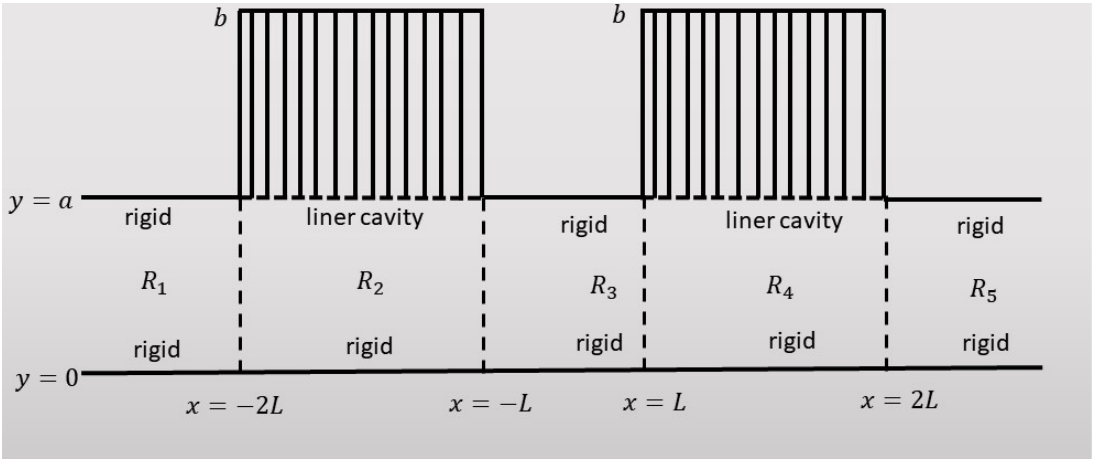

FIGURE 4.2: The physical configuration of waveguide.

The problem is made dimensionless as explained in Section 3.1. The dimensionless pressure in duct region can be written as:

$$p(x,y) = \begin{cases} p_1(x,y), & x \le -2L, \quad 0 \le y \le a, \\ p_2(x,y), & -2L \le x \le L, \quad 0 \le y \le b, \\ p_3(x,y), & x \ge -L, \quad 0 \le y \le a, \\ p_4(x,y), & -L \le x \le L, \quad 0 \le y \le b, \\ p_5(x,y), & x \ge 2L, \quad 0 \le y \le a. \end{cases} . \tag{4.64}$$

The dimensional form of boundary conditions can be written as:

$$\frac{\partial p_1}{\partial y} = 0, \qquad y = 0,\ a \qquad x \leq -2L, \tag{4.65}$$

$$\frac{\partial p_2}{\partial y} = 0, \qquad y = 0, \qquad -2L \leq x \leq -L, \tag{4.66}$$

$$\frac{\partial p_2}{\partial y} = i\omega Y(\omega) p_2(y), \qquad y = a, \quad -2L \leq x \leq -L, \tag{4.67}$$

$$\frac{\partial p_3}{\partial y} = 0, \qquad y = 0,\ a \qquad x \geq -L, \tag{4.68}$$

$$\frac{\partial p_4}{\partial y} = 0, \qquad y = 0, \qquad -L \leq x \leq L, \tag{4.69}$$

$$\frac{\partial p_4}{\partial y} = i\omega Y(\omega) p_4(y), \qquad y = a, \quad -L \leq x \leq L, \tag{4.70}$$

$$\frac{\partial p_5}{\partial y} = 0, \qquad y = 0,\ a \qquad x \geq 2L. \tag{4.71}$$

In next section the Multimodal solution of problem is explained.

4.4 Multimodal Solution

To determine the Multimodal solution, we write the pressures in duct regions as liner combination of transverse modes. Depending upon the eigenvalue problems of respective regions, the formulation of eigenvalues and transverse modes is different. The eigenvalue problems encountered in this Section are same as explained for problem 1 of this chapter. Therefore, we can write the eigenfunction expansion of regions as

$$p_1(x,y) = \sum_{n=0}^{\infty} A_{1n}\psi_n(y)e^{is_n(x+2L)} + \sum_{n=0}^{\infty} B_{1n}\psi_n(y)e^{-is_n(x+2L)}, \tag{4.72}$$

$$p_2(x,y) = \sum_{n=0}^{\infty} A_{2n}\psi_n(y)e^{i\eta_n(x+L)} + \sum_{n=0}^{\infty} B_{2n}\psi_n(y)e^{-i\eta_n(x+L)}, \tag{4.73}$$

$$p_3(x,y) = \sum_{n=0}^{\infty} A_{3n}\psi_n(y)e^{is_n(x)} + \sum_{n=0}^{\infty} B_{3n}\psi_n(y)e^{-is_n(x)}, \tag{4.74}$$

$$p_4(x,y) = \sum_{n=0}^{\infty} A_{4n}\psi_n(y)e^{i\eta_n(x-L)} + \sum_{n=0}^{\infty} B_{4n}\psi_n(y)e^{-is_n(x-L)}, \tag{4.75}$$

$$p_5(x,y) = \sum_{n=0}^{\infty} A_{5n}\psi_n(y)e^{is_n(x-2L)} + \sum_{n=0}^{\infty} B_{5n}\psi_n(y)e^{-is_n(x-2L)}. \tag{4.76}$$

Above equations in matrix form can be written as:

$$\boldsymbol{p}_1 = \boldsymbol{\psi}^t[D_1(x+2L)\boldsymbol{A}_1 + D_1(-x-2L)\boldsymbol{B}_1], \tag{4.77}$$

$$\boldsymbol{p}_2 = \boldsymbol{\psi}^t X[D_2(x+L)\boldsymbol{A}_2 + D_2(-x-L)\boldsymbol{B}_2], \tag{4.78}$$

$$\boldsymbol{p}_3 = \boldsymbol{\psi}^t[D_1(x)\boldsymbol{A}_3 + D_1(-x)\boldsymbol{B}_3], \tag{4.79}$$

$$\boldsymbol{p}_4 = \boldsymbol{\psi}^t X[D_2(x-L)\boldsymbol{A}_4 + D_2(-x+L)\boldsymbol{B}_4], \tag{4.80}$$

$$\boldsymbol{p}_5 = \boldsymbol{\psi}^t[D_1(x-2L)\boldsymbol{A}_5 + D_1(-x+2L)\boldsymbol{B}_5], \tag{4.81}$$

where $D_2(x)$ are diagonal matrix with element $e^{i\eta_n x}$, $D_1(x)$ are diagonal matrix containing element $e^{is_n x}$ and $s_n = \sqrt{K^2 - \alpha_n^2}$ are the axial wavenumber of the rigid walls bounded region

$$D_1(x) = \begin{pmatrix} e^{is_0x} & 0 & 0 & \dots & 0 & \dots \\ 0 & e^{is_1x} & 0 & \dots & 0 & \dots \\ \vdots & \vdots & e^{is_2x} & 0 & 0 & \dots \\ \vdots & \vdots & \vdots & \vdots & \vdots & \vdots \\ 0 & 0 & 0 & e^{is_nx} & 0 & \dots \\ \vdots & \vdots & \vdots & \vdots & \vdots & \vdots \end{pmatrix} \tag{4.82}$$

and

$$D_2(x) = \begin{pmatrix} e^{i\eta_0x} & 0 & 0 & \dots & 0 & \dots \\ 0 & e^{i\eta_1x} & 0 & \dots & 0 & \dots \\ \vdots & \vdots & e^{i\eta_2x} & 0 & 0 & \dots \\ \vdots & \vdots & \vdots & \vdots & \vdots & \vdots \\ 0 & 0 & 0 & e^{i\eta_nx} & 0 & \dots \\ \vdots & \vdots & \vdots & \vdots & \vdots & \vdots \end{pmatrix}. \tag{4.83}$$

Note that $\{\boldsymbol{A}_1, \boldsymbol{A}_2, \boldsymbol{A}_3, \boldsymbol{A}_4, \boldsymbol{A}_5\}$ and $\{\boldsymbol{B}_1, \boldsymbol{B}_2, \boldsymbol{B}_3, \boldsymbol{B}_4, \boldsymbol{B}_5\}$ are unknowns. We assume $\boldsymbol{B}_5 = 0$, to calculate remaining unknowns through matching the pressure and normal velocities at interfaces $x = -2L$, $x = -L$, $x = L$ and $x = 2L$. Therefore, the continuity of pressures take formulation

$$p_1(-2L, y) = p_2(-2L, y), \quad 0 \leq y \leq b, \tag{4.84}$$

$$p_2(-L, y) = p_3(-L, y), \quad 0 \leq y \leq b, \tag{4.85}$$

$$p_3(L, y) = p_4(L, y) \quad 0 \leq y \leq b \tag{4.86}$$

and

$$p_4(2L, y) = p_5(2L, y), \quad 0 \leq y \leq b, \tag{4.87}$$

respectively. The continuity of normal velocities can be given as

$$\frac{\partial p_1}{\partial x}(-2L, y) = \frac{\partial p_2}{\partial x}(-2L, y), \quad 0 \leq y \leq b, \tag{4.88}$$

$$\frac{\partial p_2}{\partial x}(-L, y) = \frac{\partial p_3}{\partial x}(-L, y), \quad 0 \leq y \leq b, \tag{4.89}$$

$$\frac{\partial p_3}{\partial x}(L, y) = \frac{\partial p_4}{\partial x}(L, y) \quad 0 \leq y \leq b \tag{4.90}$$

and

$$\frac{\partial p_4}{\partial x}(2L, y) = \frac{\partial p_5}{\partial x}(2L, y), \quad 0 \leq y \leq b. \tag{4.91}$$

Now by using (4.77)-(4.81) into (4.84)-(4.91), one may get

$$\boldsymbol{\psi}^t \left[D_1(0)\boldsymbol{A}_1 + D_1(0)\boldsymbol{B}_1\right] = \boldsymbol{\psi}^t X \left[D_2(-L)\boldsymbol{A}_2 + D_2(L)\boldsymbol{B}_2\right], \tag{4.92}$$

$$\boldsymbol{\psi}^t X \left[D_2(0)\boldsymbol{A}_2 + D_2(0)\boldsymbol{B}_2\right] = \boldsymbol{\psi}^t \left[D_1(-L)\boldsymbol{A}_3 + D_1(L)\boldsymbol{B}_3\right], \tag{4.93}$$

$$\boldsymbol{\psi}^t \left[D_1(L)\boldsymbol{A}_3 + D_1(-L)\boldsymbol{B}_3\right] = \boldsymbol{\psi}^t X \left[D_2(0)\boldsymbol{A}_4 + D_2(0)\boldsymbol{B}_4\right], \tag{4.94}$$

$$\boldsymbol{\psi}^t X \left[D_2(L)\boldsymbol{A}_4 + D_2(-L)\boldsymbol{B}_4\right] = \boldsymbol{\psi}^t \left[D_1(0)\boldsymbol{A}_5 + D_1(0)\boldsymbol{B}_5\right], \tag{4.95}$$

$$\boldsymbol{\psi}^t K_R \left[D_1(0)\boldsymbol{A}_1 - D_1(0)\boldsymbol{B}_1\right] = \boldsymbol{\psi}^t X K_y \left[D_2(-L)\boldsymbol{A}_2 - D_2(L)\boldsymbol{B}_2\right], \tag{4.96}$$

$$\boldsymbol{\psi}^t X K_Y \left[D_2(0)\boldsymbol{A}_2 - D_2(0)\boldsymbol{B}_2\right] = \boldsymbol{\psi}^t K_R \left[D_1(-L)\boldsymbol{A}_3 - D_1(L)\boldsymbol{B}_3\right], \tag{4.97}$$

$$\boldsymbol{\psi}^t K_R \left[D_1(L)\boldsymbol{A}_3 - D_1(-L)\boldsymbol{B}_3\right] = \boldsymbol{\psi}^t X K_Y \left[D_2(0)\boldsymbol{A}_4 - D_2(0)\boldsymbol{B}_4\right], \tag{4.98}$$

$$\boldsymbol{\psi}^t X K_Y \left[D_2(L)\boldsymbol{A}_4 - D_2(-L)\boldsymbol{B}_4\right] = \boldsymbol{\psi}^t K_R \left[D_1(0)\boldsymbol{A}_5 - D_1(0)\boldsymbol{B}_5\right]. \tag{4.99}$$

Multiplying (4.92)-(4.99) with $\boldsymbol{\psi}$, integrating over $y = 0$ to $y = a$, then simplifying the following equations:

$$\boldsymbol{A}_1 + \boldsymbol{B}_1 = X(D_2(-L)\boldsymbol{A}_2 + D_2(L)\boldsymbol{B}_2), \tag{4.100}$$

$$K_R(\boldsymbol{A}_1 - \boldsymbol{B}_1) = X K_Y(D_2(-L)\boldsymbol{A}_2 - D_2(L)\boldsymbol{B}_2), \tag{4.101}$$

$$X(\boldsymbol{A}_2 + \boldsymbol{B}_2) = (D_1(-L)\boldsymbol{A}_3 + D_1(L)\boldsymbol{B}_3), \tag{4.102}$$

$$X K_Y(\boldsymbol{A}_2 - \boldsymbol{B}_2) = K_R(D_1(-L)\boldsymbol{A}_3 - D_1(L)\boldsymbol{B}_3), \tag{4.103}$$

$$X(\boldsymbol{A}_4 + \boldsymbol{B}_4) = (D_1(L)\boldsymbol{A}_3 + D_1(-L)\boldsymbol{B}_3), \tag{4.104}$$

$$X K_Y(\boldsymbol{A}_4 - \boldsymbol{B}_4) = K_R(D_1(L)\boldsymbol{A}_3 - D_1(-L)\boldsymbol{B}_3), \tag{4.105}$$

$$\boldsymbol{A}_5 + \boldsymbol{B}_5) = X(D_2(L)\boldsymbol{A}_4 + D_2(-L)\boldsymbol{B}_4), \tag{4.106}$$

$$K_R(\boldsymbol{A}_5 - \boldsymbol{B}_5) = X K_Y(D_2(L)\boldsymbol{A}_4 - D_2(-L)\boldsymbol{B}_4), \tag{4.107}$$

where K_R are diagonal matrices containing the elements of axial wavenumber sn

$$K_R = \begin{pmatrix} s_0 & 0 & 0 & \dots & 0 & \dots \\ 0 & s_1 & 0 & \dots & 0 & \dots \\ \vdots & \vdots & s_2 & 0 & 0 & \dots \\ \vdots & \vdots & \vdots & \vdots & \vdots & \vdots \\ 0 & 0 & 0 & s_n & 0 & \dots \\ \vdots & \vdots & \vdots & \vdots & \vdots & \vdots \end{pmatrix} \tag{4.108}$$

and K_Y are diagonal matrices containing the elements of axial wavenumber η_n

$$K_Y = \begin{pmatrix} \eta_0 & 0 & 0 & \dots & 0 & \dots \\ 0 & \eta_1 & 0 & \dots & 0 & \dots \\ \vdots & \vdots & \eta_2 & 0 & 0 & \dots \\ \vdots & \vdots & \vdots & \vdots & \vdots & \vdots \\ 0 & 0 & 0 & s_n & 0 & \dots \\ \vdots & \vdots & \vdots & \vdots & \vdots & \vdots \end{pmatrix}. \tag{4.109}$$

Considering $\boldsymbol{B}_5 = 0$ and then comparing (4.106) with (4.107), it is straight forward to write

$$X[D_2(L)\boldsymbol{A}_4 + D_2(-L)\boldsymbol{B}_4] = K_R^{-1} X K_y [D_2(L)\boldsymbol{A}_4 - D_2(-L)\boldsymbol{B}_4]. \tag{4.110}$$

Let we define

$$F_1 = X + K_R^{-1} X K_Y \tag{4.111}$$

and

$$G_1 = X - K_R^{-1} X K_Y, \tag{4.112}$$

then (4.110) becomes

$$\boldsymbol{B}_4 = -F_1^{-1} D_2^{-1}(-L) G_1 D_2(L) \boldsymbol{A}_4. \tag{4.113}$$

By adding (4.104) and (4.105), we get

$$2D_1(L)\boldsymbol{A}_3 = F_1 \boldsymbol{A}_4 + G_1 \boldsymbol{B}_4. \tag{4.114}$$

Multiplying (4.114) with $D_1^{-1}(L)$ and using the value of $\boldsymbol{B}_4$, we get

$$2\boldsymbol{A}_3 = (F_1 D_1^{-1}(L) - G_1 D_1^{-1}(L) F_1^{-1} D_2^{-1}(-L) G_1 D_2(L))\boldsymbol{A}_4. \tag{4.115}$$

Now by subtracting (4.104) and (4.105), it is straight forward to find

$$2D_1(-L)\boldsymbol{B}_3 = G_1 \boldsymbol{A}_4 + F_1 \boldsymbol{B}_4. \tag{4.116}$$

Multiplying (4.116) with $D_1^{-1}(-L)$ and using the value of $\boldsymbol{B}_4$, we find

$$2\boldsymbol{B}_3 = (G_1 D_1^{-1}(-L) - F_1 D_1^{-1}(-L) F_1^{-1} D_2^{-1}(-L) G_1 D_2(L))\boldsymbol{A}_4. \tag{4.117}$$

By adding (4.102) and (4.103), we find

$$2\boldsymbol{A}_2 = (F_2 D_1(-L)\boldsymbol{A}_3 + G_2 D_1(L)\boldsymbol{B}_3). \tag{4.118}$$

Let we define

$$F_2 = X^{-1} + K_Y^{-1} X^{-1} K_R \tag{4.119}$$

and

$$G_2 = X^{-1} - K_Y^{-1} X^{-1} K_R. \tag{4.120}$$

Multiplying equation (4.118) with 2 and using values of $2\boldsymbol{A}_3$ and $2\boldsymbol{B}_3$, we get

$$4\boldsymbol{A}_2 = (F_2 D_1(-L) E_1 + G_2 D_1(L) E_2)\boldsymbol{A}_4. \tag{4.121}$$

Now by subtracting (4.102) and (4.103), we achieve

$$2\boldsymbol{B}_2 = (G_2 D_1(-L)\boldsymbol{A}_3 + F_2 D_1(L)\boldsymbol{B}_3). \tag{4.122}$$

Multiplying equation (4.122) with 2 and using value of $2\boldsymbol{A}_3$ and $2\boldsymbol{B}_3$, we will get

$$4\boldsymbol{B}_2 = (G_2 D_1(-L) E_1 + F_2 D_1(L) E_2)\boldsymbol{A}_4, \tag{4.123}$$

where

$$E_1 = (F_1 D_1^{-1}(L) - G_1 D_1^{-1}(L) F_1^{-1} D_2^{-1}(-L) G_1 D_2(L))$$

and

$$E_2 = (G_1 D_1^{-1}(-L) - F_1 D_1^{-1}(-L) F_1^{-1} D_2^{-1}(-L) G_1 D_2(L)).$$

Now adding (4.100) and (4.101), we find

$$2\boldsymbol{A}_1 = F_1 D_2(-L)\boldsymbol{A}_2 + G_1 D_2(L)\boldsymbol{B}_2, \tag{4.124}$$

multiplying equation (4.124) with 4 and using the value of $4\boldsymbol{A}_2$ and $4\boldsymbol{B}_2$, we get

$$8\boldsymbol{A}_1 = (F_1D_2(-L)H_1 + G_1D_2(L)H_2)\boldsymbol{A}_4. \tag{4.125}$$

Now by subtracting (4.100) and (4.101), we get

$$2\boldsymbol{B}_1 = G_1D_2(-L)\boldsymbol{A}_2 + F_1D_2(L)\boldsymbol{B}_2. \tag{4.126}$$

Multiplying (4.126) with 4 and using the value of $4\boldsymbol{A}_2$ and $4\boldsymbol{B}_2$, we get

$$8\boldsymbol{B}_1 = (G_1D_2(-L)H_1 + F_1D_2(L)H_2)\boldsymbol{A}_4, \tag{4.127}$$

where

$$H_1 = F_2D_1(-L)E_1 + G_2D_1(L)E_2$$

and

$$H_2 = G_2D_1(-L)E_1 + F_2D_1(L)E_2.$$

By adding (4.106) and (4.107), we may write

$$2\boldsymbol{A}_5 = F_1D_2(L)\boldsymbol{A}_4 + G_1D_2(-L)\boldsymbol{B}_4. \tag{4.128}$$

But on using the value of $\boldsymbol{B}_4$ from (4.113), leads to

$$2\boldsymbol{A}_5 = (F_1D_2(L) - G_1D_2(-L)F_1^{-1}D_2^{-1}(-L)G_1D_2(L))\boldsymbol{A}_4. \tag{4.129}$$

According to [70] the reflection and transmission coefficients can be written as

$$\boldsymbol{T(t)} = \frac{\boldsymbol{A}_5}{\boldsymbol{A}_1}, \tag{4.130}$$

and

$$\boldsymbol{R(r)} = \frac{\boldsymbol{B}_1}{\boldsymbol{A}_1}. \tag{4.131}$$

By using the values of $\boldsymbol{A}_5$ and $\boldsymbol{A}_1$, the transmission coefficient becomes

$$\boldsymbol{T(t)} = (F_1 D_2(L) - G_1 D_2(-L) F_1^{-1} D_2^{-1}(-L) G_1 D_2(L)) \\ (F_1 D_2(-L) H_1 + G_1 D_2(L) H_2)^{-1}. \tag{4.132}$$

Likewise on using the value of $\boldsymbol{B}_1$ and $\boldsymbol{A}_1$, we achieve the reflection coefficient as

$$\boldsymbol{R(r)} = (G_1 D_2(-L) H_1 + F_1 D_2(L) H_2)(F_1 D_2(-L) H_1 + G_1 D_2(L) H_2)^{-1}. \tag{4.133}$$

4.5 Numerical Results

In this section, the numerical results are presented. The problem is excited with the fundamental duct mode of inlet region that scatters on interaction with the lined chamber. The absolute amplitudes of first three reflected modes in inlet and the transmitted modes in outlet are plotted against frequency. These modes carry maximum of the incident energy. The main aim is to see the variation in scattering fields against frequency are connected with lined chambers. For numerical computations the speed of sound $c = 343.5$m/s,

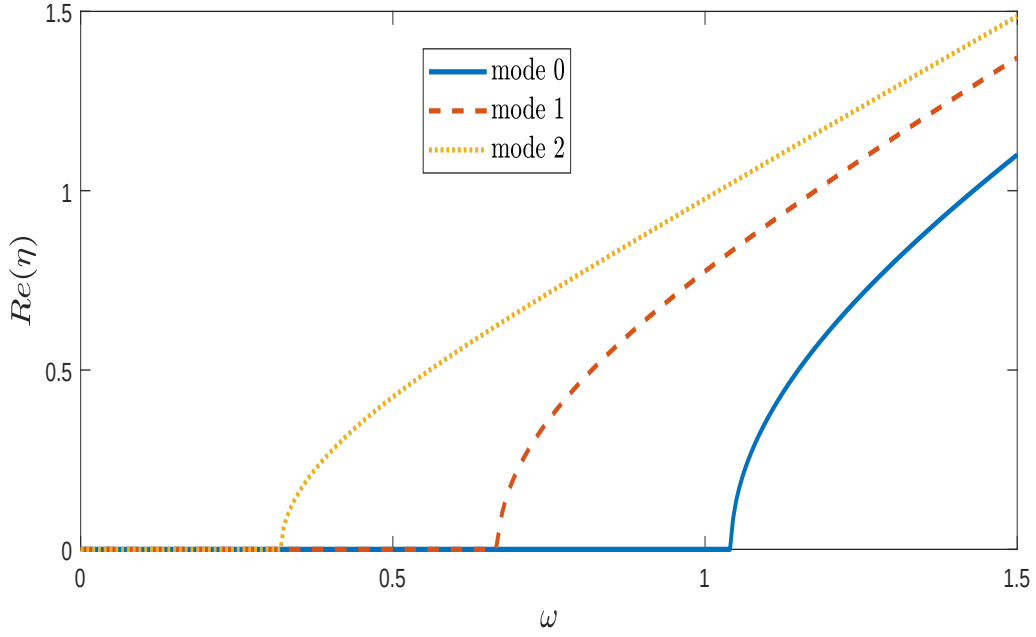

FIGURE 4.3: Trajectories of the real parts of η as a function of frequency ω.

dimensional heights $a = 25/6$ and $b = 30/6$ remain fixed. In Figs. 4.3 and 4.4, the movement of wave number of mode 0, mode 1 and mode 2 are shown against frequency ω. The real part of these modes are shown in Fig. 4.3 while imaginary parts are displayed in Fig. 4.4. The trajectories of modes wavenumber η is evident of this fact. (see Figs. 4.3-4.4).

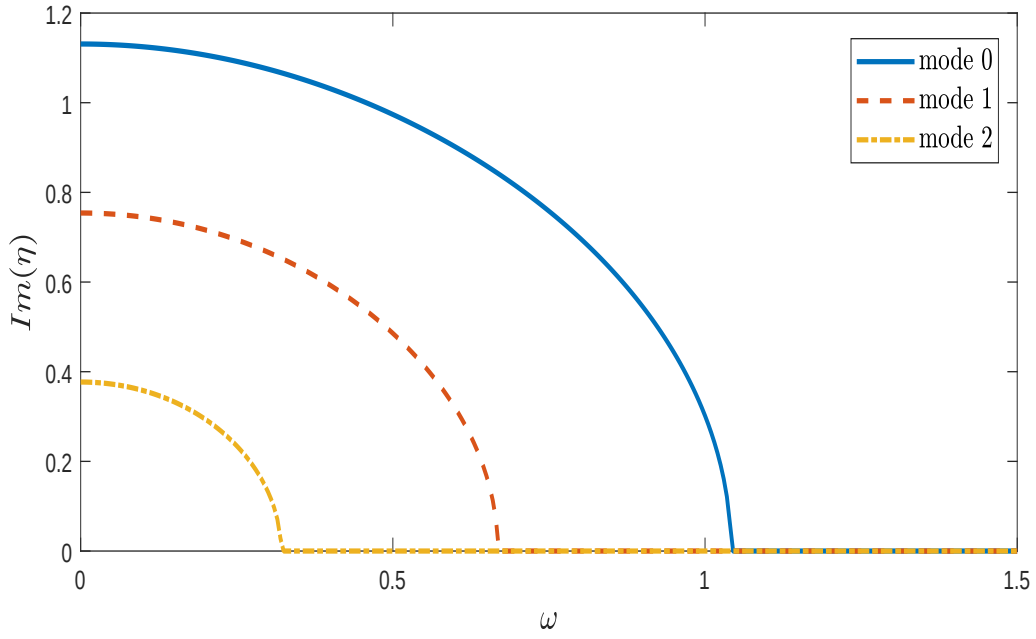

FIGURE 4.4: Trajectories of the imaginary parts of η as a function of frequency ω.

4.5.1 Scattering Amplitudes against Frequency with Single Lined Chamber

Figs. 4.5-4.10 display the scattering amplitude against frequency over $0 \leq \omega \leq 1.5$ with single lined chamber. For numerical computations the speed of sound $c = 343.5$m/s, dimensional heights $a = 25/6$ and $b = 30/6$ remain fixed. In Figs. 4.5 and 4.6, the absolute values of fundamental reflected amplitudes and fundamental transmitted amplitudes are respectively portrayed. From these graphs, it can be seen that there is huge spike between $0.3 \leq \omega \leq 0.6$ and $0.6 \leq \omega \leq 0.8$ in reflected and transmitted amplitudes respectively. The spike is because of the variation in eigenvalues.

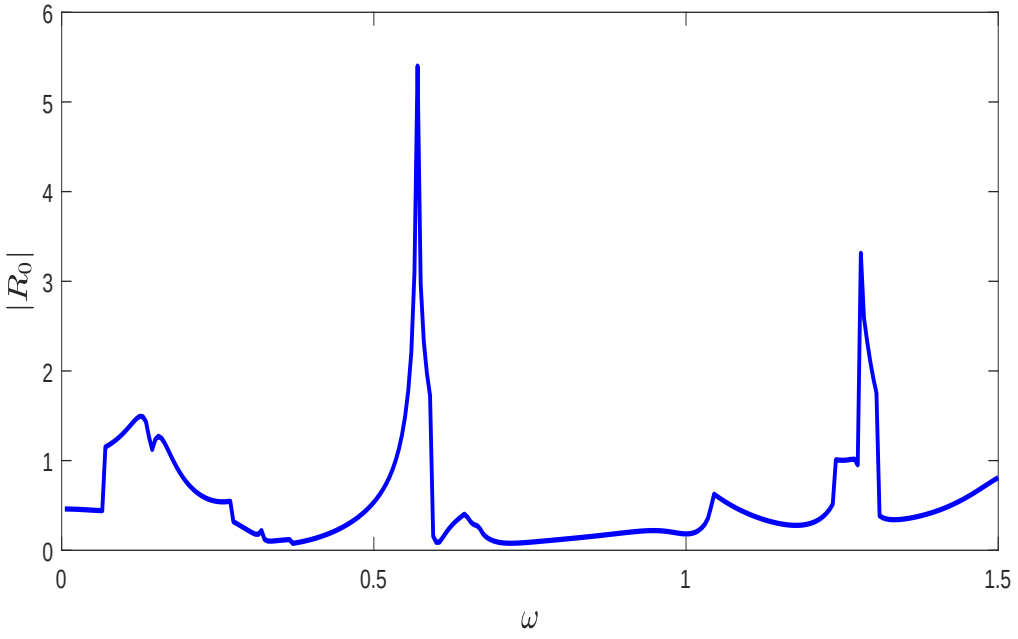

FIGURE 4.5: The absolute fundamental reflected mode $|R_0|$ against frequency ω.

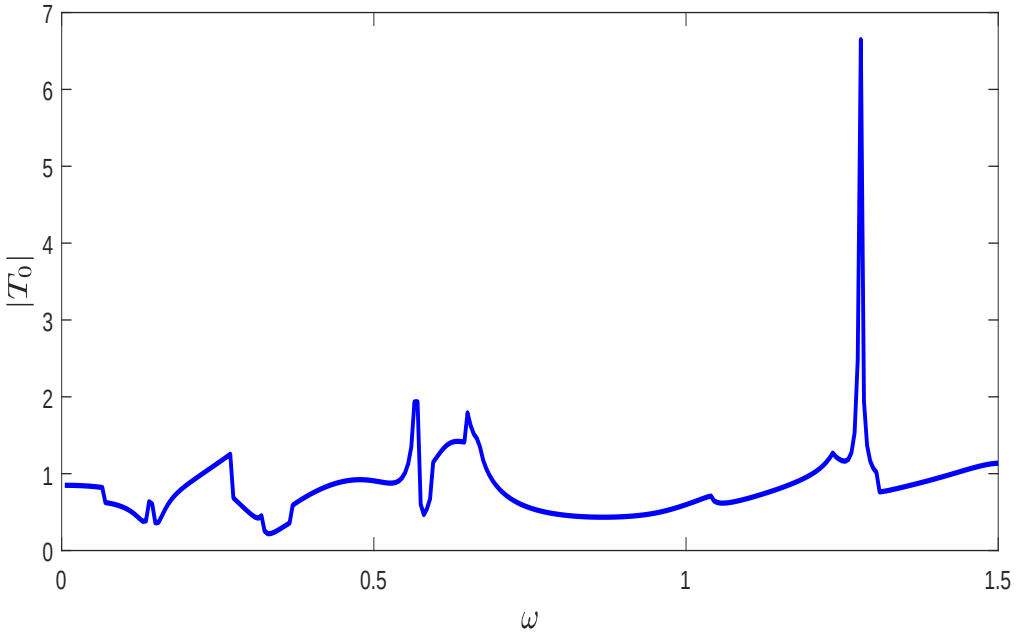

FIGURE 4.6: The absolute fundamental transmitted mode $|T_0|$ of frequency ω.

From Figs. 4.7 and 4.8, the absolute value of secondary reflected mode and absolute value of secondary transmitted mode are shown respectively.

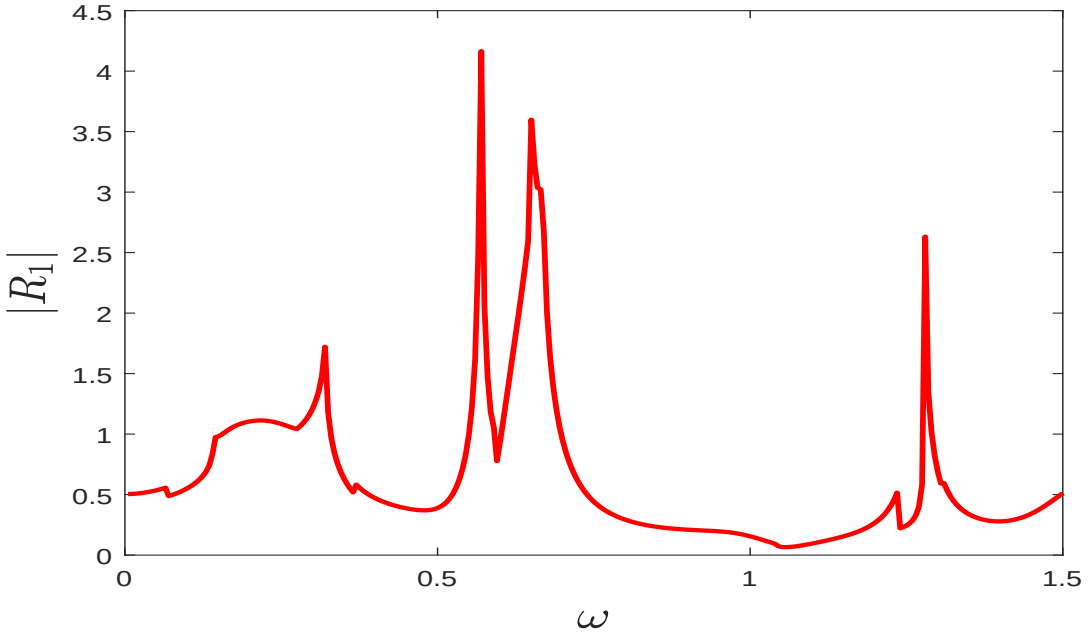

FIGURE 4.7: The absolute secondary reflected mode $|R_1|$ against frequency ω.

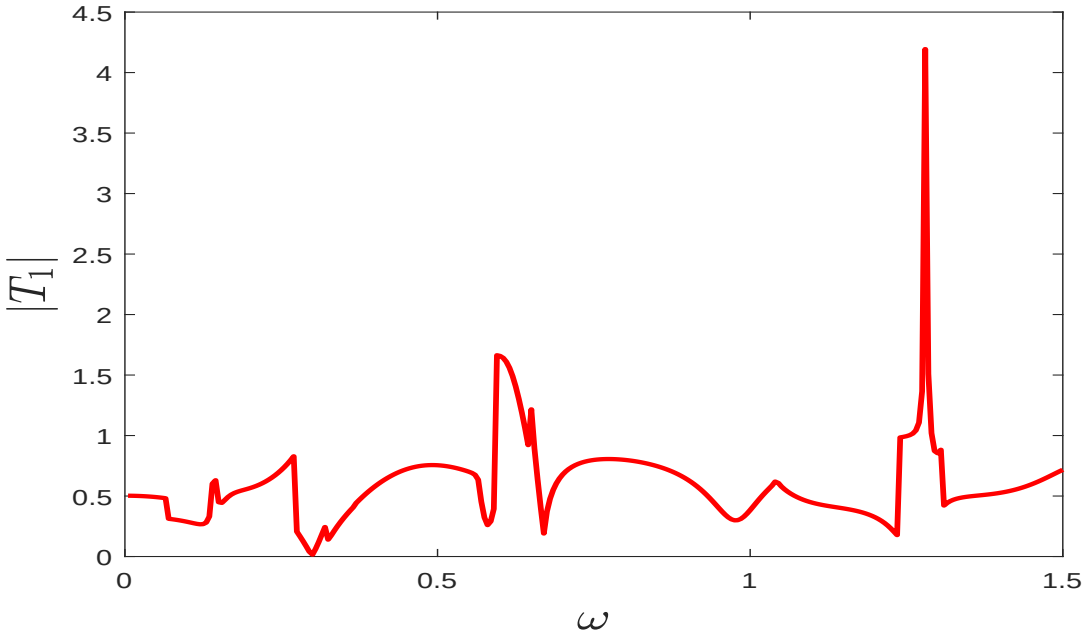

FIGURE 4.8: The absolute secondary transmitted mode $|T_1|$ against frequency ω.

It can be seen that in beginning reflected amplitude is minimum and vary on increasing frequency to its maximum value about regime $0.5 \leq \omega \leq 0.7$ whereas the transmitted amplitude spikes are $0.6 \leq \omega \leq 1.3$.

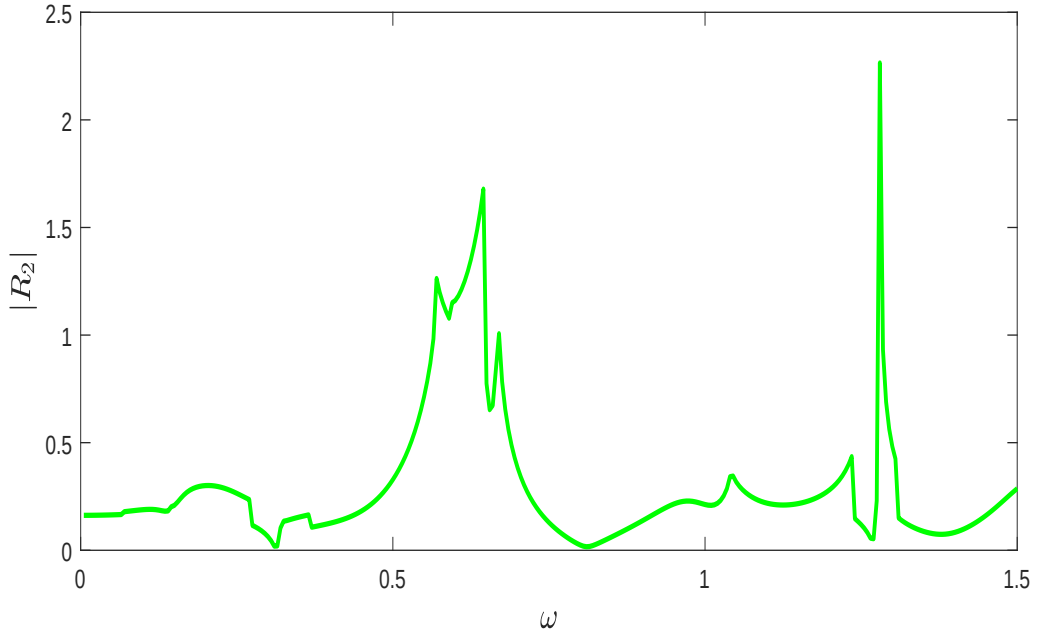

FIGURE 4.9: The absolute third reflected mode $|R_2|$ against frequency ω.

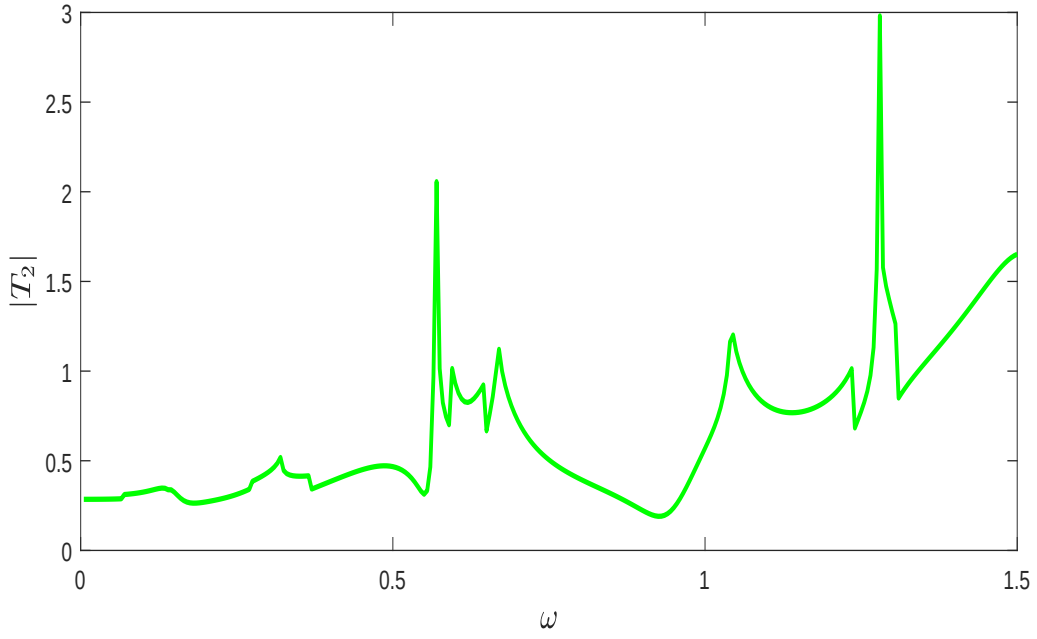

FIGURE 4.10: The absolute third transmitted mode $|T_2|$ against frequency ω.

Accordingly, in Figs. 4.9 and 4.10, the absolute value of third reflected mode and absolute value of third transmitted mode are shown respectively. It can be

seen that in beginning reflected amplitude curve is smooth but vary on increasing frequency to reach its maximum value about regime $0.6 \leq \omega \leq 1.3$ whereas, the transmitted amplitude two spikes $0.6 \leq \omega \leq 1.4$ are evident.

4.5.2 Scattering Amplitudes aginst Frequency with Double Lined Chamber

In Figs. 4.11-4.16, the absolute values of scattering amplitudes with double lined chamber are shown. The setting of involving numerical parameters is kept same with the single lined chamber. Figs. 4.11 and 4.12, depict the absolute value of fundamental reflected mode and absolute value of fundamental transmitted mode. Clearly from these graphs, one can seen a fluctuation in scattering amplitude as compared with single lined chamber. The fluctuations are caused by the addition of lined chamber.

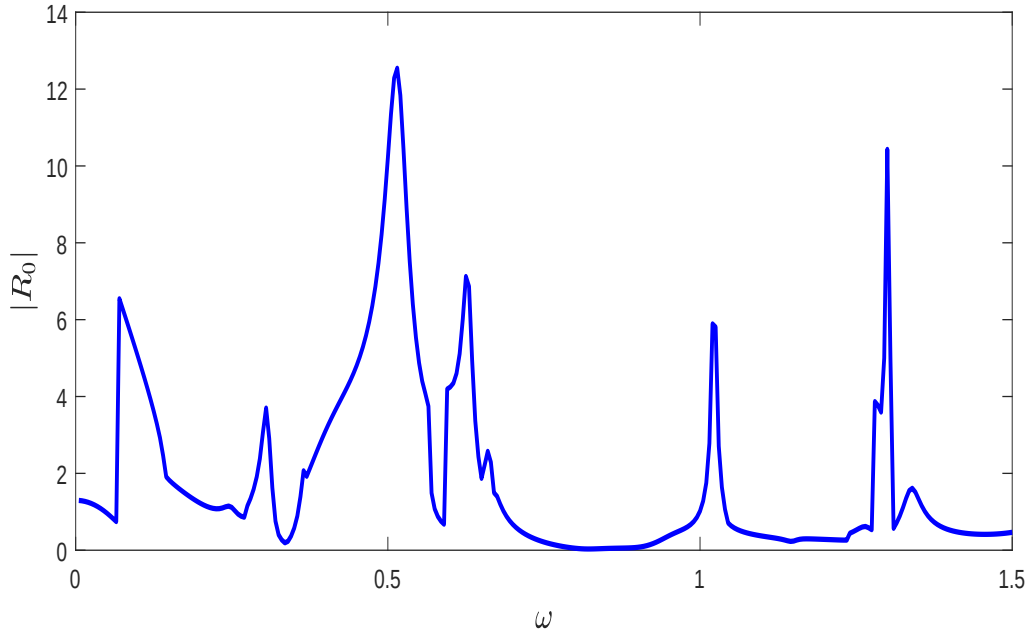

FIGURE 4.11: The absolute fundamental reflected mode $|R_0|$ against frequency ω.

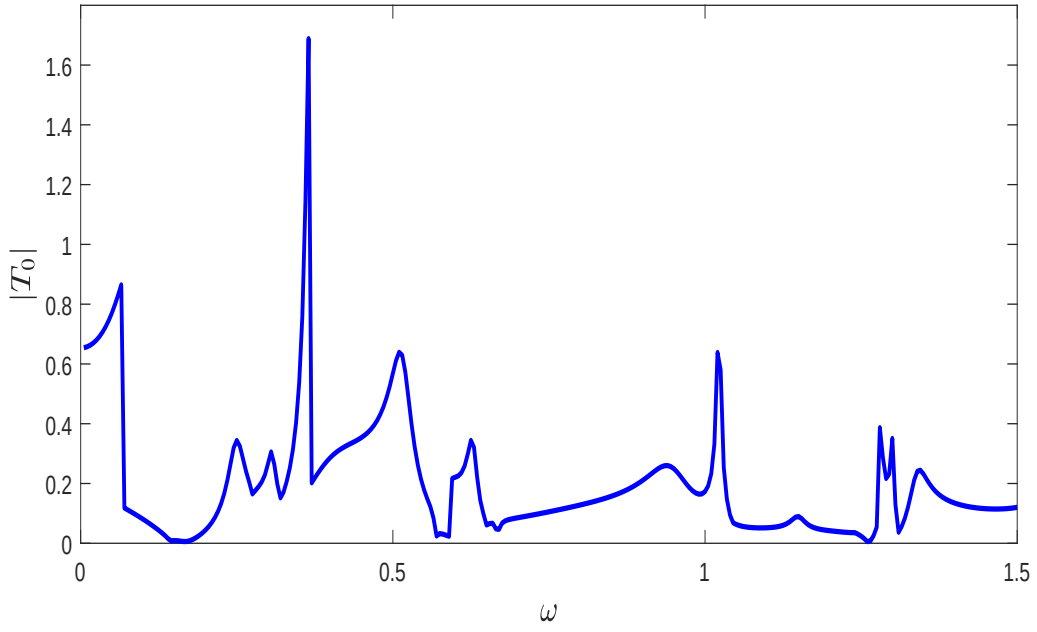

FIGURE 4.12: The absolute fundamental transmitted mode $|T_0|$ against frequency ω.

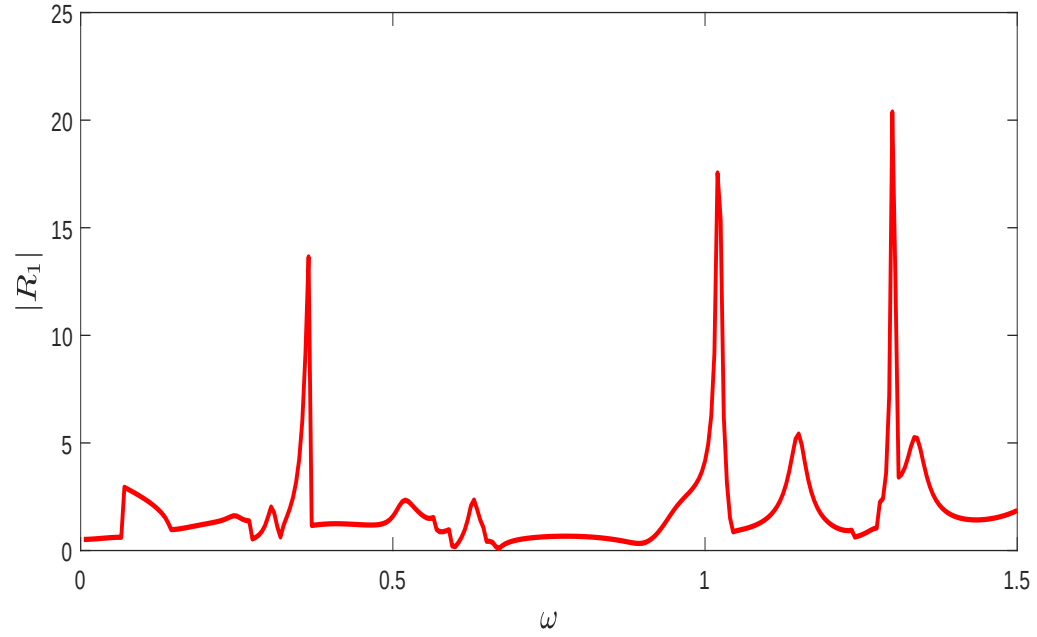

FIGURE 4.13: The absolute secondary reflected mode $|R_1|$ against frequency ω.

Figs. 4.13 and 4.14, display the absolute value of secondary reflected mode and absolute value of secondary transmitted mode are shown respectively. It can be

seen that there is a little variation in scattering graphs with double lined chamber when compared with single lined chamber graphs against frequency.

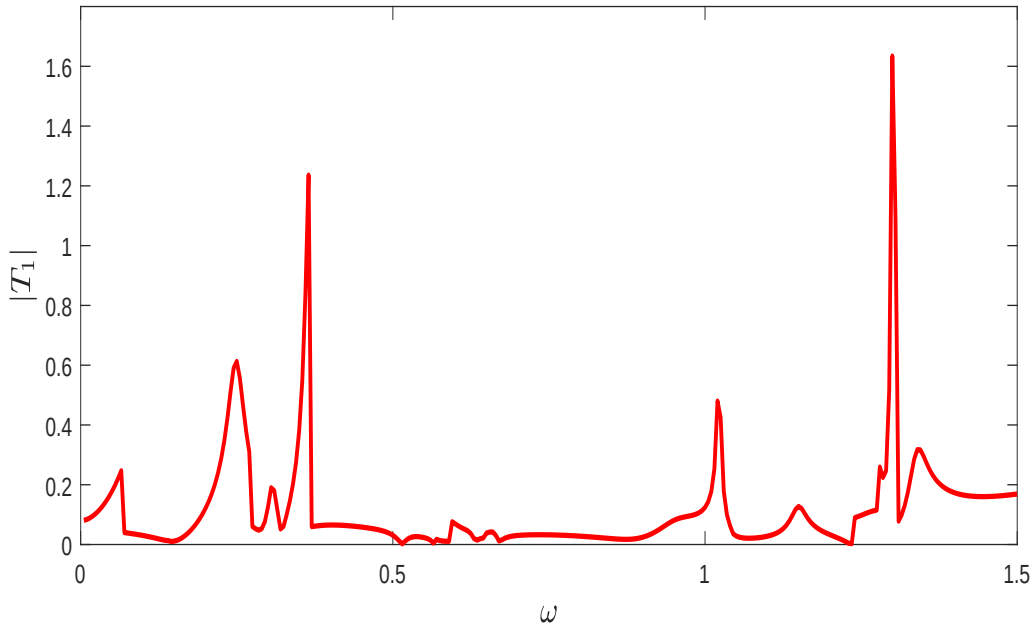

FIGURE 4.14: The absolute secondary transmitted mode $|T_1|$ against frequency ω.

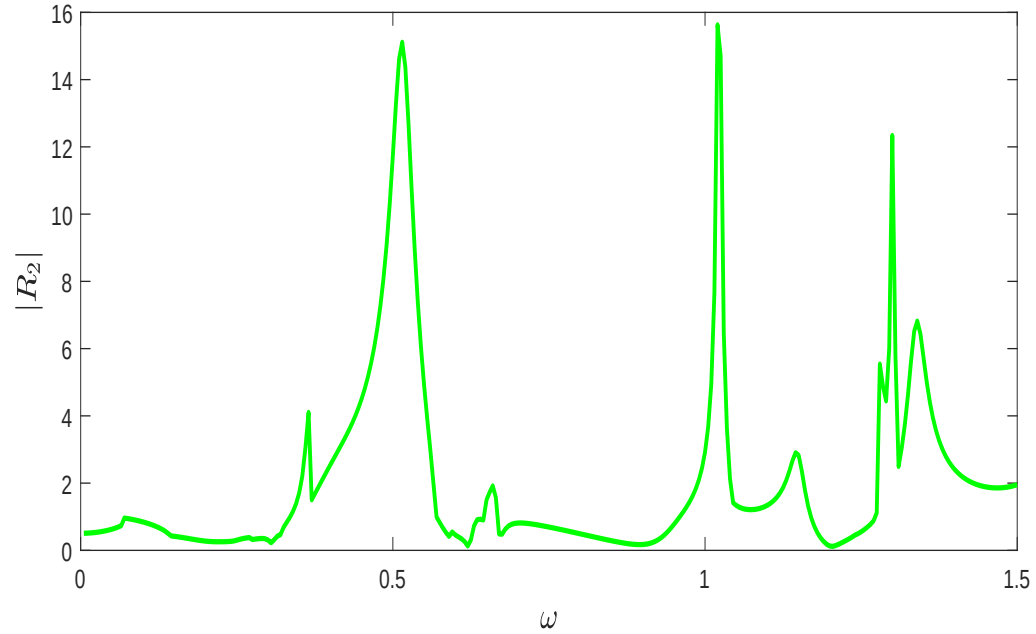

FIGURE 4.15: The absolute third reflected mode $|R_2|$ against frequency ω.

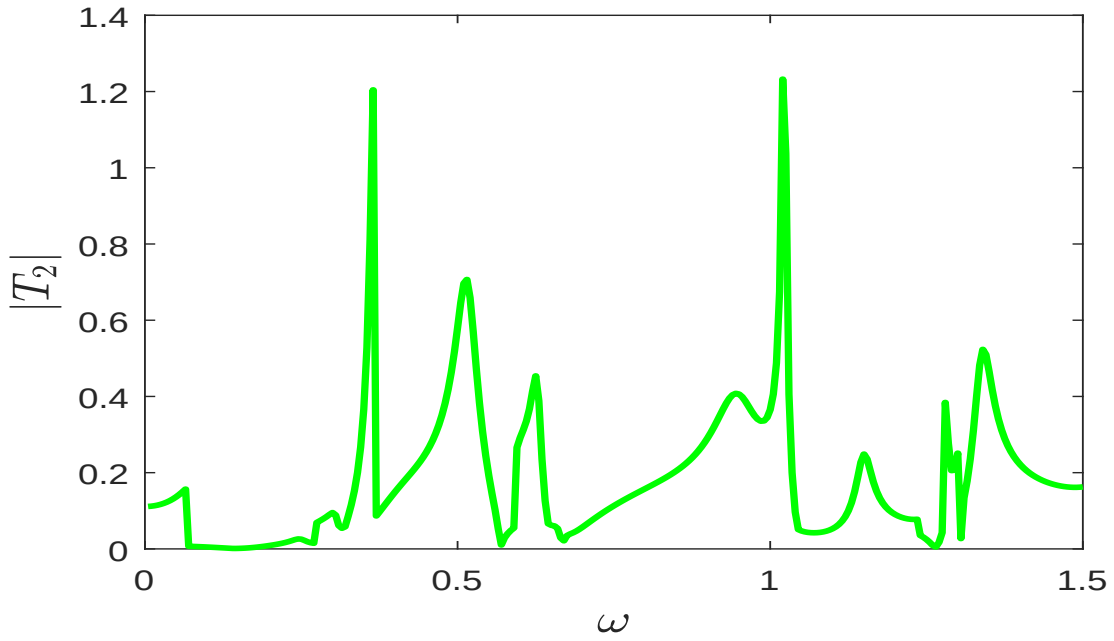

FIGURE 4.16: The absolute third reflected mode $|T_2|$ against frequency ω.

In Figs. 4.15 and 4.16, the absolute value of third reflected mode and absolute value of third transmitted mode are shown. Accordingly to secondary mode graphs, there is a little impact of double lined chamber on the third modes.

Chapter 5

Summary and Conclusion

The current study presents scattering analysis of inclusion of single and double lined chamber cavities in an infiniet waveguide. The Multimodal technique is applied to solve the boundary value problems. This technique is initially described by prototype problems then is further applied to solve the liner cavity problems. Therefore two prototype problems exited by the plane piston which lies along the terminating vertical of duct are discussed in Chapter 3. First problem is bounded by rigid walls while the later problem comprises liners along the upper horizontal wall. Both of these problems are governed with Helmholtz's equation and contained boundary conditions to be rigid-rigid and rigid-impedance typed. The Multimodal solution is sorted by projecting the travelling wave modes with orthogonal basis of rigid walls bounding segment and rigid impedance walls segment. The numerical results shows the effect of trajectories of eigenmodes on wave propagating against the velocity of the plane piston. From these results, it is found that by changing the value of velocity of the moving piston a variation in fundamental, secondary and third mode propagation obtained. The scattering from expansion chamber with single and double lined cavities are discussed in Chapter 4. The Multimodal solution for both problems is achieved through the projection of orthogonal basis of respective regions. The absolute amplitudes of reflected and transmitted fields are plotted against frequency. Only first three modes are plotted since most of energy is carried out through these modes. The sound attenuation

with single and double lined chamber cavities are discussed. These problems are radiated by the fundamental duct mode of incident region which passes through the ancheotic region after interaction with the chamber cavities. From numerical results, it is found that the inclusion of double liner cavities changes the position of spikes appearing in the scattering amplitudes as well as increases the intensity of sound attenuation.

Bibliography

[1] R. Mangiarotty, Acoustic-lining concepts and materials for engine ducts, The Journal of the Acoustical Society of America, 48(3): 783-794 (1970).

[2] W. Bi, V. Pagneux, D. Lafarge and Y. Auregan, Sound propagation in non-uniform lined duct by the multimodal method, Proceeding of 10th International Conference on Sound and Vibration, 3229-3236 (2003).

[3] J. Allard and N. Atalla, Propagation of sound in porous media: modelling sound absorbing materials, John Wiley and Sons (2009).

[4] M. Ayub, R. Nawaz and A. Naeem, Diffraction of sound waves by a finite barriers in a moving fluid, Journal of Mathematical Analysis and Applications, 349(1): 245-258 (2009).

[5] M. Ayub, R. Nawaz and A. Naeem, Line source diffraction by a slit in a moving fluid, Canadian Journal of Physics, 87(11): 1139-1149 (2009).

[6] M. Ayub, R. Nawaz and A. Naeem, Diffraction of an impulsive line source with wake, Physica Scripta, 82(4): 045402 (2010).

[7] M. Ayub, A. Naeem and R. Nawaz, Sound due to an impulsive line source, Computer and Mathematics with Applications, 60(12): 3123-3129 (2010).

[8] R. Nawaz, A note on acoustic diffraction by an absorbing finite strip, Indian Journal of Pure and Applied Mathematics, 43(6): 571-589 (2012).

[9] R. Nawaz and M. Ayub, An exact and asymptotic analysis of a diffraction problem, Meccanics, 48(3): 653-662 (2013).

[10] R. Nawaz and M. Ayub, Closed form solution of electromagnetic wave diffraction problem in a homogeneous bi-isotropic medium, Mathematical Methods in the Applied Science, 38: 176-187 (2014).

[11] R. Nawaz, A. Naeem and M. Ayub, Point source diffraction by a slit in a moving fluid, Waves in Random and Complex Media, 24(4): 357-375 (2014).

[12] R. Nawaz, M. Ayub and A. Javaid, Plane wave diffraction by a fnite plate with impedance boundary conditions , Plos One, 9(4): e92566 (2014).

[13] R. Nawaz, A. Wahab and A. Rasheed, An intermediate range solution to a diffraction problem with impedance conditions, Modern Optics, 61(16): 1324-1332 (2014).

[14] A. Wahab and R. Nawaz, A note on noise source localization, Vibration and Control, 22(7): 1889-1894 (2016).

[15] M. H. Tiwana, Rab Nawaz, A. B. Mann, Radiation of sound in a semi infinite hard duct inserted axially into a larger infinite lined duct , Analysis and Mathematical Physics, 016-0154-4, s13324 (2017).

[16] M. U. Hassan, M. Naz and R. Nawaz, Reflected Field Analysis of Soft-Hard1 Pentafurcated Waveguide, Advances in Mechanical Engineering, 9(2): 1687814017692697 (2017) .

[17] K. Peat, The acoustical impedance at the junction of an extended inlet or outlet duct, Journal of Sound and Vibration, 150(1): 101-110 (1991).

[18] B. Regan and J. Eaton, Modelling the influence of acoustic liner non-uniformities on duct modes, Journal of Sound and Vibration, 219(5): 859-879 (1999).

[19] T. Elandy, H. Boden and R. Glav, Application of the point matching method to model circumferentially segmented non-locally reacting liners, 7th AIAA/CEAS Aeroacoustics Conference and Exhibit, 2202 (2001).

[20] S. Felix and V. Pagneux, Sound propagation in rigid bends: A multimodal approach, The Journal of the Acoustical Society of America, 110(3): 1329-1337 (2001).

[21] W. Bi, V. Pagneux, D. Lafarge and Y. Auregan, Modelling of sound propagation in a non-uniform lined duct using a multi-modal propagation method, Journal of Sound and Vibration, 289(4-5): 1091-1111 (2006).

[22] Y. Auregan and M. Lerous, Experimental evidence of an instability over an impedance wall in a duct with flow, Journal of Sound and Vibration, 317(3-5): 432-439 (2008).

[23] D. Marx, Y. Auregan, H. Bailliet and J. C. Valiere, Piv and ldv evidence of hydrodynamic instability over a liner in a duct with flow, Journal of Sound and Vibration, 329(18): 3798-3812 (2006).

[24] E. L. Shenderov, Helmholtz equation solution corresponding to multilpe roots of the dispersion equation for a waveguide with impedance walls, Acoustical physics, 46(3): 357-363 (2006).

[25] R. Kirby, P. Williams and J. Hill, A comparison between the performance of different silencer designs for gas turbine exhaust systems, (2012).

[26] F. D. Denia, A. Selamet, M. J. Martínez and F. J. Fuenmayor, Sound attenuation of a circular multi-chamber hybrid muffler, Noise control engineering journal, 56(5): 356-364 (2008).

[27] M. Abom, Derivation of four-pole parameters including higher order mode effects for expansion chamber mufflers with extended inlet and outlet, Journal of Sound and Vibration, 137(3): 403-418 (1990).

[28] R. I. Nuruddeen, R. Nawaz and Q. M. Z. Zia, Dispersion of Elastic Waves in an Asymmetric Three-Layered Structure in the Presence of Magnetic and Rotational Effects, Progress In Electromagnetics Research M, 91: 165-177 (2020).

[29] R. I. Nuruddeen, R. Nawaz and Q. M. Z. Zia, Asymptotic analysis of an anti-plane shear dispersion of an elastic

five-layered structure amidst contrasting properties, Arch Appl Mech, 90: 1875-1892 (2020).

[30] R. I. Nuruddeen, R. Nawaz and Q. M. Z. Zia, Investigating the viscous damping effects on the propagation of Rayleigh waves in a three-layered inhomogeneous plate, Physica Scripta, 95(065224): 1-11 (2020).

[31] R. I. Nuruddeen, R. Nawaz and Q. M. Z. Zia, Effects of thermal stress, magnetic field and rotation on the dispersion of elastic waves in an inhomogeneous five- layered plate with alternating components, Science Progress, 103(3): 1-22 (2020).

[32] R. I. Nuruddeen, R. Nawaz and Q. M. Z. Zia, An asymptotic investigation of the dynamics and dispersion of an elastic five-layered plate for anti-plane shear vibration, Journal of Engineering Mathematics, 128(1): 1-12 (2021).

[33] R. I. Nuruddeen, R. Nawaz and Q. M. Z. Zia, Asymptotic approach to anti-plane dynamic problem of asymmetric three-layered composite plate, Mathematical Methods in the Applied Sciences, 44(14): 10933-10947 (2021).

[34] A. Cummings and I. J. Chang, Sound attenuation of a finite length dissipative flow duct silencer with internal mean flow in the absorbent, Journal of Sound and Vibration, 127(1): 1-17 (1988).

[35] M. B. Xu, A. Selamet, I. J. Lee and N. T. Huff, Sound attenuation in dissipative expansion chambers, Journal of Sound and Vibration, 272(3): 1125-1133 (2004).

[36] A. Selamet, M. B. Xu, I. J. Lee and N. T. Huff, Analytical approach for sound attenuation in perforated dissipative silencers, The Journal of the Acoustical Society of America, 115(5): 2091-2099 (2004).

[37] R. Nawaz and J. B. Lawrie, Scattering of a fluid-structure coupled wave at a flanged junction between two flexible waveguides, The Journal of the Acoustical Society of America, 134(3): 1939-1949 (2013).

[38] R. Nawaz, M. Afzal and M. Ayub, Acoustic propagation in two-dimensional waveguide for membrane bounded ducts, Communications in Nonlinear Science and Numerical Simulation, 20(2): 421-433 (2015).

[39] M. Afzal, R. Nawaz and A. Ullah, Attenuation of dissipative device involving coupled wave scattering and change in material properties, Applied Mathematics and Computation, 290: 154-163 (2016).

[40] T. Nawaz, M. Afzal and A.Wahab, Scattering analysis of a flexible trifurcated lined waveguide structure with step-discontinuities, Physica Scripta, 96(11): 115004 (2021).

[41] M. Afzal, T. Nawaz and R. Nawaz, Scattering characteristics of planar trifurcated waveguide structure containing multiple discontinuities, Waves in Random and Complex Media, 1-20 (2020).

[42] M. Afzal, S. Shafique and A. Wahab, Analysis of traveling waveform of flexible waveguides containing absorbent material along flanged junctions, Communication in Non-Linear Science and Numerical Simulation, 97: 105737 (2021).

[43] M. Afzal and S. Shafique, Attenuation analysis of flexural modes with absorbent lined flanges and different edge conditions, Journal of the Acoustical Society of America, 148: 85 (2020).

[44] S. Shafique, M. Afzal and R. Nawaz, On the attenuation of fluid-structure coupled modes in a non-planar waveguide, Mathematics and Mechanics of Solids, 25(10): 1-20 (2020).

[45] M. Afzal, J. U. Satti and R. Nawaz, Scattering characteristics of non-planar trifurcated waveguides, Meccanica, 55: 977-988 (2020).

[46] T. Nawaz, M. Afzal and R. Nawaz, The scattering analysis of trifurcated waveguide involving structural discontinuities, Advances in Mechanical Engineering, 11(7): 1-11 (2019).

[47] H. Bilal and M. Afzal, Acoustic wave scattering from a wave-bearing cavity in a rectangular waveguide, Journal of the Acoustical Society of America, 144: 1681 (2018).

[48] A. Ullah, R. Nawaz and M. Afzal, Fluid-structure coupled wave scattering in a flexible duct at the junction of planar discontinuities, Advances in Mechanical Engineering, 9(7): 1-11 (2017).

[49] S. Shafique, M. Afzal and R. Nawaz, On mode matching analysis of fluid-structure coupled wave scattering between two flexible waveguides, Canadian Journal of Physics, 95(6): 581-589 (2017).

[50] J. B. Lawrie and M. Afzal, Acoustic scattering in a waveguide with a height discontinuity bridged by a membrane: a tailored Galerkin approach, Journal of Engineering Mathematics, 105(1): 99-115 (2017).

[51] J. B. Lawrie, Comments on a class of orthogonality relations relevant to fluid-structure interaction, Meccanica, 47(3): 783-788 (2012).

[52] L. Huang, Modal analysis of a drumlike silencer, The Journal of the Acoustical Society of America, 112(5): 2014-2025 (2002).

[53] J. U. Satti, M. Afzal and R. Nawaz, Scattering analysis of a partitioned wave-bearing cavity containing different material properties, Physica Scripta, 94(11): 115-223 (2019).

[54] S. W. Rienstra, A classification of duct modes based on surface waves, Wave Motion, 37(2): 119-135 (2003).

[55] E. J. Brambley and N. Peake, Classification of aeroacoustically relevant surface modes in cylindrical lined ducts, Wave Motion, 43(4): 301-310 (2006).

[56] M. Hassan and A. D. Rawlins, Sound radiation in a planar trifurcated lined duct, Wave Motion, 29(2): 157-174 (1999).

[57] M. Ayub, M. H. Tiwana and A. B. Mann, Acoustic diffraction in a trifurcated waveguide with mean flow, Communications in Nonlinear Science and Numerical Simulation, 15(12): 3939-3949 (2010).

[58] X. Wang and C. M. Mak, Wave propagation in a duct with a periodic Helmholtz resonators array, The Journal of the Acoustical Society of America, 131(2): 1172-1182 (2012).

[59] M. Afzal, R. Nawaz, M. Ayub and A. Wahab, Acoustic scattering in flexible waveguide involving step discontinuity, PloS one, 9(8): e103807 (2014).

[60] A. H. Nayfeh, J. E. Kaiser and D. P. Telionis, Acoustics of aircraft engine duct systems, AJAA Journal, 13(2): 130-153 (1975).

[61] A. D. Rawlins, Radiation of sound from an unflanged rigid cylindrical duct with an acoustically absorbing internal surface, Proceedings of the Royal Society of London. A. Mathematical and Physical Sciences, 361(1704): 65-91 (1978).

[62] M. Ayub, M. H. Tiwana and A. B. Mann, Influence of the dominant mode propagation in a trifurcated lined duct with different impedances, Physica Scripta, 81(3): 035402 (2010).

[63] J. B. Lawrie and I. D. Abrahams, An orthogonality relation for a class of problems with high-order boundary conditions; applications in sound-structure interaction, The Quarterly Journal of Mechanics and Applied Mathematics, 52(2): 161-181 (1999).

[64] M. Afzal and J. U. Satti, The traveling wave formulation of a splitting chamber containing reactive components, Archive of Applied Mechanics, 91(5): 1959-1980 (2021).

[65] L. E. Kinsler, A. R. Frey, A. B. Coppens and J. V. Sanders, Hand book, Fundamental of acoustics, 4th Edition, Wiley (1999).

[66] G. Stokes, On the theories of the internal friction of fluids in motion and of the equilibrium and motion of elastic solids, Transactions of the Cambridge Philosophical Society, 8: 75-102 (1845).

[67] V. Galanenko, On coupled modes theory of two-dimensional wave motion in elastic waveguides with slowly varying parameters in curvilinear orthogonal coordinates, The Journal of the Acoustical Society of America, 103(4): 17521762 (1998).

[68] V. Pagneux and A. Maurel, Lamb wave propagation in elastic waveguides with variable thickness, Proceedings of the Royal Society A: Mathematical, Physical and Engineering Sciences, 462(2068): 1315-1339 (2006).

[69] L. Tang and J. Cheng, Numerical analysis on laser-generated guided elastic waves in a hollow cylinder, Journal of nondestructive evaluation, 21(2): 35-53 (2002).

[70] L. Xiong, Use of mode coupling to enhance sound attenuation in acoustic ducts: effects of exceptional point, (2016).